



**GEOLOGICAL SURVEY OF CANADA  
OPEN FILE 7227**

**Physical Property Measurements at the GSC Paleomagnetism  
and Petrophysics Laboratory, including Electric Impedance  
Spectrum Methodology and Analysis**

**R.J. Enkin, D. Cowan, J. Tigner, A. Severide, D. Gilmour,  
A. Tkachyk, M. Kilduff, B. Vidal, J. Baker**

**2012**



Natural Resources  
Canada

Ressources naturelles  
Canada

**Canada**



**GEOLOGICAL SURVEY OF CANADA  
OPEN FILE 7227**

## **Physical Property Measurements at the GSC Paleomagnetism and Petrophysics Laboratory, including Electric Impedance Spectrum Methodology and Analysis**

**R.J. Enkin<sup>1</sup>, D. Cowan<sup>2</sup>, J. Tigner<sup>2</sup>, A. Severide<sup>2</sup>, D. Gilmour<sup>2</sup>, A. Tkachyk<sup>3</sup>,  
M. Kilduff<sup>2</sup>, B. Vidal<sup>2</sup>, J. Baker<sup>1</sup>**

<sup>1</sup> Geological Survey of Canada - Pacific, PO Box 6000, Sidney, BC V8L 4B2

<sup>2</sup> University of Victoria, PO Box 1700 Stn CSC, Victoria BC V8W 2Y2

<sup>3</sup> Royal Roads University, 2005 Sooke Road, Victoria, BC V9B 5Y2

**2012**

©Her Majesty the Queen in Right of Canada 2012

doi:10.4095/291564

This publication is available for free download through GEOSCAN (<http://geoscan.ess.nrcan.gc.ca/>).

**Recommended citation:**

Enkin, R.J., Cowan, D., Tigner J., Severide, A., Gilmour, D., Tkachyk, A., Kilduff, M., Vidal, B., and Baker, J., 2012. Physical Property Measurements at the GSC Paleomagnetism and Petrophysics Laboratory, including Electric Impedance Spectrum Methodology and Analysis; Geological Survey of Canada, Open File 7227, 42 p., doi:10.4095/291564

## Table of Contents

1. Introduction . . . . .	1
2. Samples. . . . .	1
3. Density and Porosity. . . . .	2
4. Magnetic Properties. . . . .	4
a. <i>Magnetic Susceptibility</i> . . . . .	4
b. <i>Magnetic Remanence and Koenigsberger Ratio</i> . . . . .	8
c. <i>Rock Magnetism Measurements</i> . . . . .	10
5. Electrical Properties. . . . .	11
6. Summary. . . . .	18
References . . . . .	19
Table 1: GSC GanFeld lithological classification scheme (after Shimamura et al., 2008) .	20
Table 2: Mira Geoscience lithological classification scheme (after Parsons et al., 2009) . .	36

### List of Figures:

- 1: Drilling subsample cores
- 2: Density histogram from the British Columbia Rock Property Database
- 3: Chamber for vacuum impregnation of 5 subsamples
- 4: Immersed mass measurement using a laboratory-designed Jolly balance
- 5: Magnetic susceptibility histogram from the British Columbia Rock Property Database
- 6: GF Instruments SM20 magnetic susceptibility meter
- 7: Sapphire Instruments SI2B susceptibility meter
- 8: Density - magnetic susceptibility biplot from the British Columbia Rock Property Database
- 9: Agico JR5-A Spinner Magnetometer
- 10: Magnetic remanence - magnetic susceptibility biplot.
- 11: J-Meter Coercivity Spectrometer
- 12: LabView program JMP to analyze the J-Meter Coercivity Spectrometer output
- 13: Day plot (biplot of magnetic hysteresis ratios) of the Great Bear Iron Oxide Copper Gold (IOCG) database
- 14: Bartington MS2WF Thermomagnetic Susceptibility Meter
- 15: LabView program Xo(T) to analyze Bartington Thermomagnetic Susceptibility Meter output
- 16: Time evolution of the resistivity of 5 rock samples and their immersion water
- 17: Electrode connections for rock electrical impedance measurements.
- 18: Solartron 1260 Frequency Response Analyzer
- 19: LabView program ZARCFIT for analysis of electrical impedance spectra
- 20: Pelton et al. (1978) model of a mineralized rock and its equivalent electric circuit as a “Zarc”
- 21: Equivalent circuits for analyzing rock impedance
- 22: Relationship between magnetic susceptibility, density and electrical resistivity in the Great Bear-IOCG database
- 23: Electrical resistivity - chargeability biplot of the British Columbia and Great Bear-IOCG database

**Glossary of Terms:**

$m_D$  – dry mass [g] (dry sample)

$m_I$  - immersed mass [g] (sample immersed under water)

$m_S$  - saturated mass [g] (sample saturated with water)

$P$  - porosity (proportion of the volume which is not occupied by rock minerals)

$V_G$  - geometric volume [cm<sup>3</sup>] (including pore space)

$V_S$  - skeletal volume [cm<sup>3</sup>] (excluding connected porosity)

$\rho_B$  - bulk density [g/cm<sup>3</sup>] (density including porosity)

$\rho_S$  - skeletal density [g/cm<sup>3</sup>] (density of rock forming minerals)

$H_C$  - coercive force [A/m] (or  $\mu_0 H_C$  [T]) (magnetic backfield after saturation which reduces magnetization to zero)

$H_{CR}$  - remanent coercive force [A/m] (or  $\mu_0 H_{CR}$  [T]) (magnetic backfield after saturation which produces zero magnetization on removal of field)

$K_N$  - Koenigsberger ratio [unitless] (natural remanent magnetization divided by the induced magnetization in geomagnetic field)

$M_I$  - induced magnetism [A/m] (reversible magnetization of a sample in an external magnetic field)

$M_{RS}$  - remanence of saturation [A/m] (magnetization after sample subjected to large magnetic field)

$M_S$  - saturation magnetization [A/m] (ferromagnetic magnetization while sample subjected to large magnetic field)

$NRM$  - natural remanent magnetization [A/m] (permanent magnetization)

$T_C$  - Curie temperature [°C] (temperature at which ferromagnetism ceases)

$\chi_0$  - magnetic susceptibility [unitless, (A/m)/(A/m)] (per volume ratio of a rock's reversible magnetization to a small applied external magnetic field)

$C$  - capacitance [F] (a circuit element that stores electrical charge)

EIS - electrical impedance spectrum

$f$  - linear frequency [Hz = s<sup>-1</sup>]

$M_0$  - initial chargeability [unitless or mV/V] (instantaneous drop in voltage after the current is removed in IP survey)

$M_X$  - Newmont standard chargeability [ms] (integration of voltage from 430 to 1100 ms after the current is removed normalized to peak voltage in IP survey)

$Z$  - Electrical impedance [ $\Omega$ ] (complex electrical resistance as a function of frequency, where the real part is related to energy loss and the complex part is related to energy storage)

$Z_{arc}$  - the electrical impedance response of a resistor in parallel with a constant phase element

$Z_{CPE}$  - constant phase element impedance [ $\Omega$ ] (a distributed circuit element with properties between those of a resistor and a capacitor)

$\rho$  - electrical resistivity [ $\Omega m$ ] (= resistance [ $\Omega$ ] times the geometric factor = sample area / sample length)

$\omega$  - angular frequency [s<sup>-1</sup>]

## 1. Introduction

Measurement of the physical properties of rocks provides the link between the two dominant activities in mineral exploration: geological mapping and geophysical surveys. Geological mapping reveals the distribution of rocks and their alteration zones on the surface and in drill cores. Geophysical surveys locate the 3-dimensional distribution of physical properties, which are proxies for the ore bodies, their host lithologies and their cover. Gravity surveys depend on contrasts in density. Magnetic surveys image variations in magnetic susceptibility and remanence. A wide range of electrical and electromagnetic methods locate rocks of different electrical resistivity and chargeability.

To identify the geological sources of geophysical anomalies it is necessary to ascertain the physical property fingerprints of each rock type and each formation. It is also useful to compile a physical properties database to address several issues. For example, what are the spatial variations of both mean values and their dispersions? How do alteration processes modify physical properties and how can this information be exploited to provide vectors to economic deposits? Where are the geophysically imageable contrasts? What techniques should be applied to optimize geophysical surveys and their interpretation?

The Geological Survey of Canada - Pacific Division houses its Paleomagnetism and Petrophysics Laboratory (PPL) at the Pacific Geoscience Centre in Sidney, British Columbia. Physical properties of rocks measured in the PPL are reported as data spreadsheets (Enkin, et al., 2008) and incorporated in other data portals such as the Rock Property Database System hosted by Mira Geoscience <http://rpds.mirageoscience.com/>.

This document provides a brief description of the methods used in the PPL to measure density, magnetic properties and electric properties, and information helpful to the interpretation and application of the data it produces. There is particular emphasis on new methods and analysis techniques for electrical impedance spectra, in order to produce reliable measurements of

electrical resistivity and chargeability.

## 2. Samples

Most samples analyzed in the PPL are hand samples or pieces of exploration core submitted by collaborating geologists. It is important to consider the location distribution of samples. Some regions have excellent coverage due to the availability of suitable outcrops and recent geological activity that led to the sampling. The sampling, however, is never uniform. Mappers do not collect samples on the basis of the area they represent, but rather they attempt to sample the range of available rock types. Exotic occurrences will be selected whereas the host rocks will only occasionally induce additional sampling. Extra sampling is particularly frequent on altered or mineralized rocks, which are the main target for geophysical surveys precisely because of their rarity. Furthermore, the three-dimensional nature of stratigraphy means that spatial averaging over two dimensions will necessarily lead to misleading interpretations. It is thus essential, when compiling spatial and lithological mean values, to consider the appropriate weighting for each sample and, furthermore, to group them correctly together.

Along with the original identification, each sample is given a PPL number consisting of 2 letters corresponding to the Provincial or Territorial postal abbreviation (e.g., BC for British Columbia, NT for the Northwest Territories) and 5 digits assigned sequentially. An upcoming goal is to have the PPL samples and results entered into the Geological Survey of Canada Sample Management System (SMS), where they are assigned a "Curation Number" and an "SMS ID". The SMS provides the opportunity to link physical properties data to all other field and lab data associated with the sample. All samples are photographed before processing.

In order to get full value out of the database, every sample must also have its corresponding metadata - specifically its location and lithology. Lithologies are difficult to summarize as the specific descriptors used for any suite of samples depends on the geological context and the particular focus of the geologists concerned.



**Figure 1:** Drilling 2.5 cm diameter subsample cores from a hand sample or exploration core.

Whatever information is submitted with the samples is included in the results spreadsheet as an unformatted text entry. It is important, however, to establish a restricted set of standard lithologies in order to organize the results. As a compromise in the continual tension between “lumping” and “splitting”, we use two classification schemes. First, we apply the Geological Survey of Canada lithological scheme established for field mappers using the GanFeld system, Table 1 (Shimamura, et al., 2008).

Second, we use the much more restricted Mira Geoscience “Master Lithology” classification scheme developed by their employee Sharon Parsons, Table 2 (Parsons et al., 2009). Both schemes use a 3-level hierarchy, but whereas the GSC scheme attempts to capture the specific details of any field situation and is allowed to expand, the Mira Geoscience scheme is fixed at 126 distinct lithologies. No system is ideal for all applications, but we find the Mira Geoscience scheme allows for rapid, useful comparison of results from disparate sources of samples.

A useful hand sample for physical properties work is dominantly unweathered, and at least 5 cm across its smallest dimension in order to allow subsampling of representative rock. Core subsamples are drilled with a 2.5 cm diameter water-cooled diamond bit, and cut to ~2.2 cm-long right-cylinders (Fig. 1). Efforts are made to pick a representative sub-sample of the hand

specimen and to avoid drilling through pre-existing planes of weakness in the rock. Samples are drilled perpendicular to stratification or foliation in order to sample all minerals contained in the rock sample and thus provide a better understanding of the bulk properties. However, oriented samples are cored perpendicular to the oriented surface. For particular cases, rectangular prisms are cut to allow studies of anisotropy. Once the core sample has been cut to length, the flat ends are smoothed using a lapidary disk sander.

If necessary, skeletal density and magnetic susceptibility can be measured on a whole hand sample or on bags of unconsolidated grains.

### 3. Density and Porosity

Density, the mass per unit volume ( $\text{g/cm}^3$ ), is the physical property determined by gravity surveys. Density provides the most direct proxy for the degree of mineralization as most ore minerals are significantly denser than the silicates which dominate unmineralized rocks (Fig. 2). Permeability and weathering influence porosity which affects density.

In the PPL, sample volume is determined in two ways. The geometric volume ( $V_G$ ) which includes the pore space and the skeletal volume ( $V_S$ ) which excludes connected porosity. For  $V_G$ , the core diameter and length is measured with calipers (to 0.1 mm). Formulae for missing wedges or sides help estimate the volume of imperfect cylinders. The geometric volume is accurate to about 3% for typical samples around 11 cm<sup>3</sup> in volume, as long as the sample is sufficiently cylindrical.

Before the wet mass and skeletal volume is measured, the dry mass ( $m_D$ ) is measured using an analytical balance (to 0.1 mg). Freshly cut samples are typically left to dry for a day or more before this step, and a vacuum oven is available for special cases. Because gravity anomalies are almost always produced by rocks sitting below the water table, the dry mass density is seldom required for geophysical analysis.

The skeletal volume ( $V_S$ ) is measured using

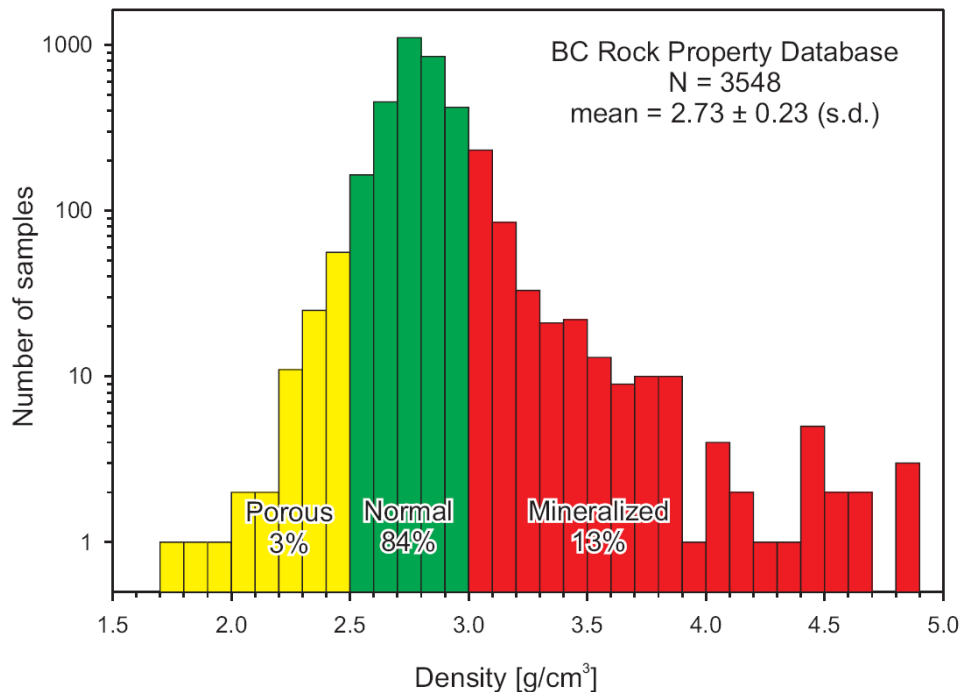


**Figure 2:** Density histogram from the British Columbia Rock Property Database.



**Figure 3:** Chamber for vacuum impregnation of 5 subsamples.

Archimedes' principle (weight in air - weight in water) using a specially built Jolly balance (Jolly, 1864). In order to completely saturate the samples with water, samples are placed in 50 mL

beakers, 5 at a time, in a specially designed chamber (Fig. 3). Under vacuum ( $< 5$  kPa) to void the rock pore space of as much gas as possible, the beakers are filled three-quarters full with water. After bubbles stop streaming from the samples (at least 10 minutes), the vacuum pump is turned off and the beakers are removed. Distilled water is used as part of the subsequent electrical measurements (see Section 5, below), and the samples sit in their beakers for 24 to 36 hours before the next measurements are done.

Each sample is removed from its beaker with metal tweezers and the outside is dried with a KimWipe<sup>®</sup>. Tweezers are used to avoid affecting the electrical conductivity of the beaker water. It is important that the only water in the sample be contained within the pore space and not on the surface and that pore water is not removed via exposure or capillary action during the drying process.

The saturated mass ( $m_s$ ) of the sample is measured on the pan of the analytical balance, and then the sample is placed in a wire basket suspended under the pan (Fig. 4). The sample's beaker with its original soaking water is lifted into place to immerse the sample, and the immersed mass ( $m_l$ ) is measured. Note that the immersed mass also includes the buoyancy of the wire



**Figure 4:** The immersed mass ( $m_i$ ) of a sample being measured by suspension in a beaker of water below a balance, using a laboratory-designed Jolly balance.

basket, requiring a small but near-constant correction.

The skeletal density ( $\rho_S$ ) refers to the density of rock forming minerals and is defined as the immersed mass divided by the skeletal volume:

$$[\text{eq.1}] \quad \rho_S = m_S / ((m_S - m_I) / \rho_W),$$

where  $\rho_W$  is the density of water at the measurement temperature. The bulk density ( $\rho_B'$ ) is the saturated mass divided by the geometric volume:

$$[\text{eq.2}] \quad \rho_B' = m_S / V_G.$$

More accurately, the geometric volume is equivalent in principle to the skeletal volume plus the pore volume derived from the difference in mass before and after the water saturation:

$$[\text{eq.3}] \quad \rho_B = m_S / ((m_S - m_I) + (m_S - m_D)) / \rho_W.$$

For standard samples, the uncertainties are about 2% for  $\rho_S$  and  $\rho_B$ , and 6% for  $\rho_B'$ .

The connected porosity ( $P$ ) is the proportion of the volume which is not occupied by rock minerals:

$$[\text{eq.4}] \quad P = (m_S - m_D) / (m_S - m_I).$$

If the dry mass ( $m_D$ ) was not measured, the porosity can be calculated using the geometric volume through the bulk density (eq. 2) for a less accurate measurement:

$$[\text{eq.5}] \quad P' = (\rho_S - \rho_B') / \rho_S.$$

As the porosity is derived from the difference of two similar numbers, an absolute rather than relative uncertainty is quoted. When the dry mass,  $m_D$ , is available,  $P$  (eq. 4) is precise to  $\pm 0.002$  (i.e., 0.2 percentage points), whereas  $P'$  calculated using equation 5 is only good to  $\pm 0.02$ .

#### 4. Magnetic Properties

Magnetic survey anomalies arise from contrasts in the magnetization of rock bodies. The two magnetization mechanisms are induction (reversible magnetization when an external magnetic field such as the geomagnetic field is applied) and remanence (permanent magnetism acquired during the formation of the rock or during subsequent events such as hydrothermal alteration).

##### 4a. Magnetic Susceptibility

Magnetic susceptibility ( $\chi_0$ ) is the per volume ratio of a rock's reversible magnetization to a small applied external magnetic field. While susceptibility is a dimensionless quantity, it is useful to think of the SI units of magnetic susceptibility as (A/m)/(A/m). Note that it is smaller in CGS units by an order of magnitude (precisely a factor  $4\pi$ ) because of a different set of equations used to describe magnetization and magnetic fields.

It is distressing how often published reports neglect to state the units of magnetic susceptibility, nor even the assumed power of 10. In the absence of units, one has to resort to *a priori* knowledge of reasonable magnetic susceptibility ranges (Fig. 5). Equant magnetite grains have a theoretical maximum magnetic susceptibility of 3 SI (Néel, 1955) and rock magnetic measurements show that it is very rare to have susceptibilities above 5 SI (Heider, et al., 1996). Mafic rocks, which typically host a few percent magnetite by volume, usually have susceptibilities in the  $10^{-2}$  SI range, while sediments and felsic rocks usually have susceptibilities in the  $10^{-4}$  SI range. Pure quartz or carbonates are diamagnetic, that is they get



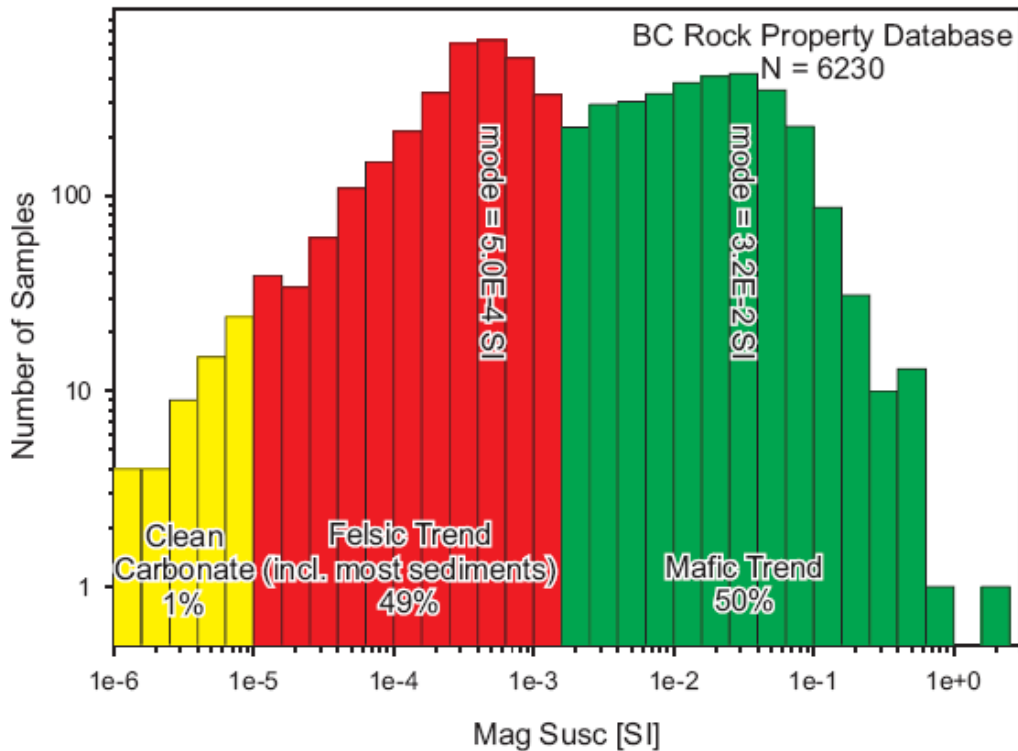


Figure 5: Magnetic susceptibility histogram from the British Columbia Rock Property Database.



Figure 6: GF Instruments SM20 Magnetic Susceptibility Meter.

magnetized antiparallel to the external field, but never with susceptibility below  $-15 \times 10^{-6}$  SI. Small concentrations of clastic input often bring carbonate susceptibilities up to  $10^{-5}$  SI. Large negative susceptibilities are certainly contaminated by electric currents in electric conductors due to Faraday’s law of induction. If a

data table of magnetic susceptibilities does not fit these expected ranges, then the units must be suspected to have been incorrectly reported. In the PPL, magnetic susceptibilities are reported in per volume SI units.

The magnetic susceptibility of hand samples is measured with a GF Instruments SM20 magnetic susceptibility meter, distributed by ASC Scientific (Fig. 6). The unit, which operates at 10 kHz and has a 5 cm diameter coil, is ideal for field measurements. If a hand sample is less than 5 cm thick, then the observed susceptibility is low. Hand sample susceptibility is only reported in our summary tables when it is impossible to subsample, for example if the sample is too friable.

Subsample cores are measured with a Sapphire Instruments SI2B susceptibility meter (Fig. 7). Its high operating frequency, 19.2 kHz, offers high sensitivity but has a smaller skin-depth in samples with high electrical conductivity. Thus it is important that samples are well dried before measurement. The SI2B is calibrated for an assumed volume of sample, so the values quoted are corrected for the true volume of the sample.

Note that magnetic susceptibility values are

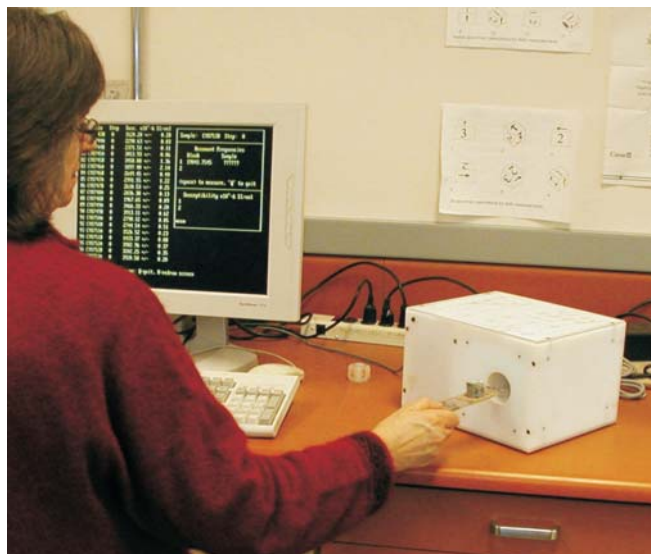


**Figure 7:** Saphire Instruments SI2B Susceptibility Meter

dominated by the concentrations of the minor accessory iron oxide and sulphide minerals, which vary significantly through an outcrop and even within a hand sample. Even though an individual measurement will have an uncertainty of better than 1%, natural variations of a factor 2 or 3 are expected on the cm-size scale, and order-of-magnitude variations are almost always observed across an outcrop.

The biplot of magnetic susceptibility against density almost always reveals two clusters, both showing magnetic susceptibility increasing with density, but one band with susceptibility between  $10^{-4}$  and  $10^{-3}$  SI, and the second between  $10^{-2}$  and  $10^{-1}$  SI (Fig. 8). This rarely reported observation was discussed by Henkel (1991, 1994) who called the lower one the “biotite amphibole paramagnetic trend” and the higher one the “magnetite trend”. We observe that magnetite concentration is the dominant source of magnetic susceptibility in both bands, so we call the lower one the “felsic trend” and the upper one the “mafic trend”. Note that mafic minerals rarely survive the erosion and transportation mechanisms which lead to sedimentary rocks, so most sedimentary rocks fall within the felsic trend.

#### 4b. Magnetic Remanence and Koenigsberger Ratio

Magnetic anomalies are almost always interpreted first as spatial variations in magnetic susceptibility, and the magnetic remanence is usually only considered when no reasonable interpretation can be proposed without it. Two notable examples of magnetic remanence dominating the magnetic surveys are the mid-oceanic stripes parallel to ocean ridges from where new crust spreads, and the point-like anomalies associated with kimberlite pipes. Whereas induced magnetization is nearly parallel to the external field, magnetic remanence can point in any direction.

The PPL is equipped to perform full paleomagnetic studies on collections of oriented rocks, with applications to paleogeography, deformation history, the dating of hydrothermal events, and magnetostratigraphic dating. For petrophysical work, it is useful to measure the magnitude of natural magnetic remanence (NRM) even for unoriented samples.

Magnetic remanence is measured on an Agico JR5-A spinner magnetometer (Fig. 9), using the standard core subsamples. The JR5-A has a sensitivity of  $10^{-5}$  A/m. As with the susceptibility measurements, the remanence is corrected for the volume of the sample.

One important complication is that samples dominated with iron oxides, such as iron formations, can get magnetized during sampling. The effect can be highlighted by simply tapping the sample with a hammer and re-measuring to observe if there is change caused by piezomagnetic remanence. In such cases, a more realistic measure of the natural remanence is made by first performing a gentle alternating field demagnetization step of 2 mT maximum intensity. We use a Schonstedt GSD-5 alternating field demagnetizer with 2-axis tumbler.

The Koenigsberger ratio ( $K_N$ ) is the natural remanent magnetization divided by the induced magnetization:

$$[\text{eq.6}] \quad K_N = NRM / \chi_0 H_0,$$

where  $H_0 = B_0/\mu_0$  is the strength of the geomagnetic field. The units of  $H_0$  are A/m, but the geomagnetic field strength is usually quoted

as magnetic induction ( $B_0$ ) with units of Tesla (T). The conversion factor is the permittivity of free space,  $\mu_0=4\pi\times 10^{-7}$  A/(m T). For comparing the efficiency of magnetization among different rocks, the Koenigsberger ratio is reported using a standard field of  $B_0 = 50$  mT, however for more accurate magnetic anomaly interpretation, it is important to use the local geomagnetic field strength, which in Canada varies from 51 to 60 mT (<http://ngdc.noaa.gov/wist/magfield.jsp>).

Most rocks have a Koenigsberger ratio below 1 (Fig. 10). This observation is often used as justification for not including magnetic remanence in magnetic survey interpretations. Nevertheless, it is impossible to know how big the influence of remanence can be without measuring it on rock samples. When a significant proportion of rocks from a region display high Koenigsberger ratios, then magnetic remanence plays an important role.

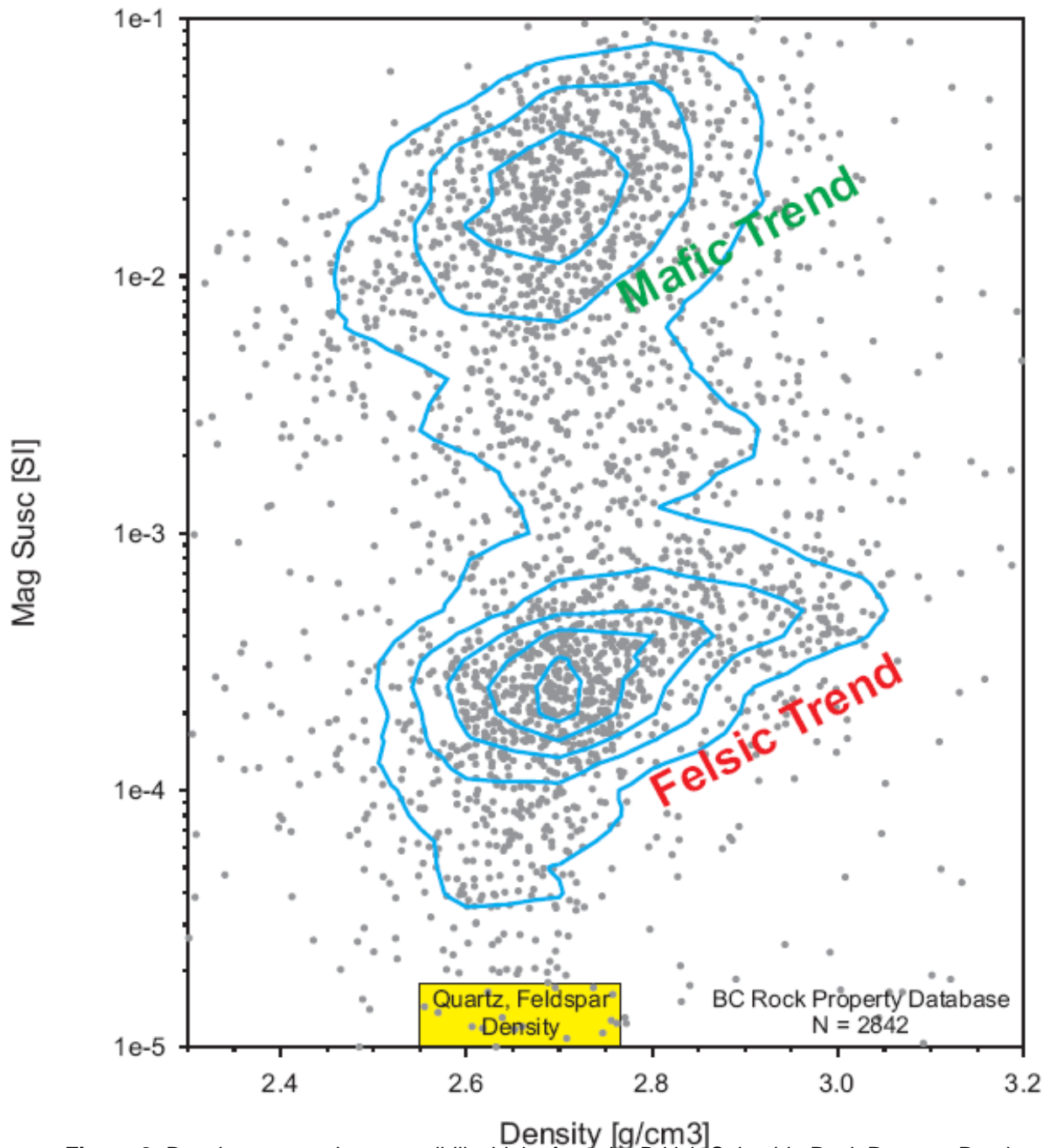
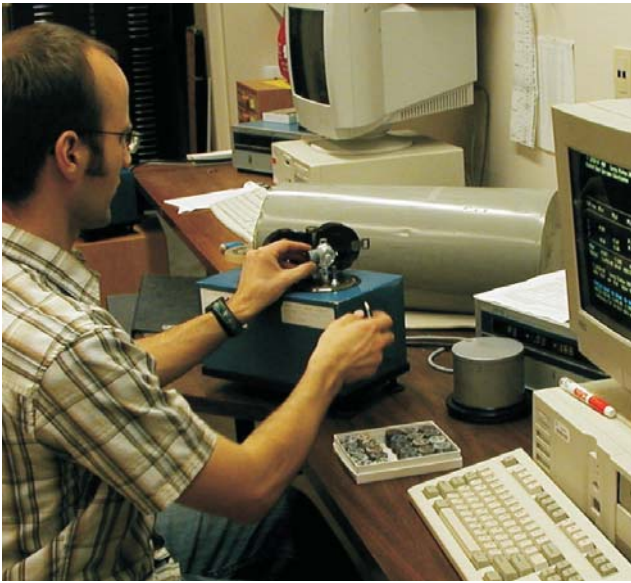


Figure 8: Density - magnetic susceptibility biplot from the British Columbia Rock Property Database.



**Figure 9:** Agico JR5-A Spinner Magnetometer for measuring magnetic remanence.

#### 4c. Rock Magnetism Measurements

Detailed rock magnetic measurements efficiently reveal useful information concerning the iron oxides and sulphides which record many aspects of a rock's geological history. In sedimentary rocks, the magnetic minerals fingerprint different sedimentary sources. In mineralized rocks, they reflect the oxygen fugacity of hydrothermal fluids. Rock magnetic studies are designed to determine the mineralogical compositions, grain sizes and concentrations of magnetic grains.

The J-Meter Coercivity Spectrometer (Fig. 11) is designed for studying ferromagnetic minerals contained in rocks and sediments by simultaneously measuring magnetic hysteresis cycles and isothermal remanence magnetization (IRM) curves (Enkin, et al., 2007). Rock chips (~1 to 2 g) are placed in a 7mm×10mm×22mm

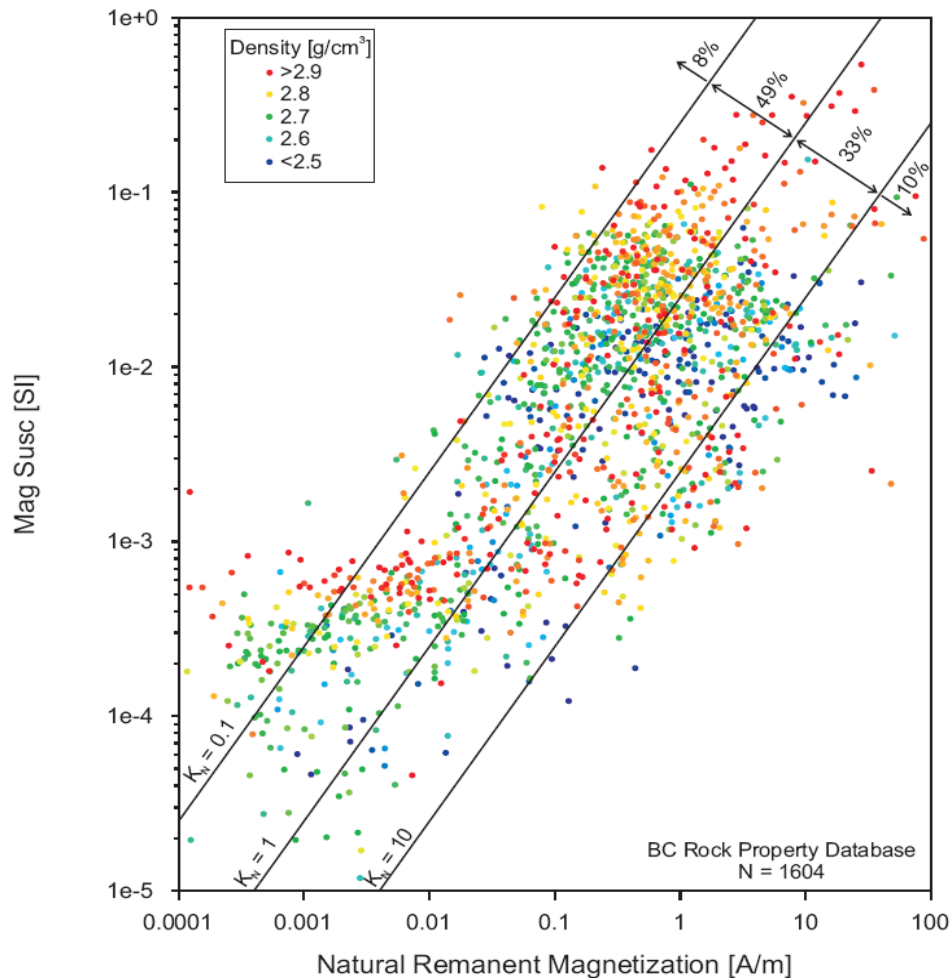


**Figure 10:** Magnetic remanence - magnetic susceptibility biplot from the British Columbia Rock Property Database, displaying lines of equal Koenigsberger ratio. The colours display density variations.

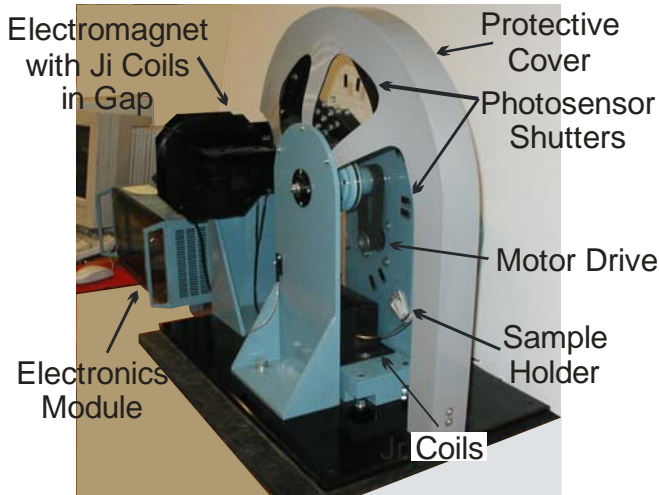


Figure 11: J-Meter Coercivity Spectrometer

box and packed with cotton to immobilize them. The box is inserted in a sample holder on the edge of the 50 cm diameter acrylic disk of the coercivity spectrometer. The disk spins at 17.5 Hz through the pole pieces of an electromagnet. With each rotation the induced magnetism ( $M_I$ ) of the sample is measured with secondary coils

within the pole pieces, and the remanence ( $M_R$ ) is measured by a set of coils placed in a mu-metal magnetic shield. The magnetic field is ramped slowly up to 500 mT, and then down to the opposite polarity, -500 mT, making virtually continuous recordings of the hysteresis cycle ( $M_I(H)$ ) and the IRM acquisition and re-magnetization curves ( $M_R(H)$ ). The sensitivity of the  $M_R$  channel of the J-Meter is about  $10^{-3}$  A/m, while the sensitivity of the  $M_I$  channel is only about  $10^{-1}$  A/m because of the impossibility of damping out vibrations in the electromagnet. Each run takes only about 6 minutes, making the J-Meter an extremely efficient method to study many samples.

The LabView program JMP has been developed in house to analyze the J-Meter output (Fig. 12). In particular, the standard hysteresis parameters of saturation magnetization ( $M_S$ ), remanence of saturation ( $M_{RS}$ ), coercive force ( $H_C$ ), and the remanent coercive force ( $H_{CR}$ ) are used to produce a Day plot (Day, et al., 1977;

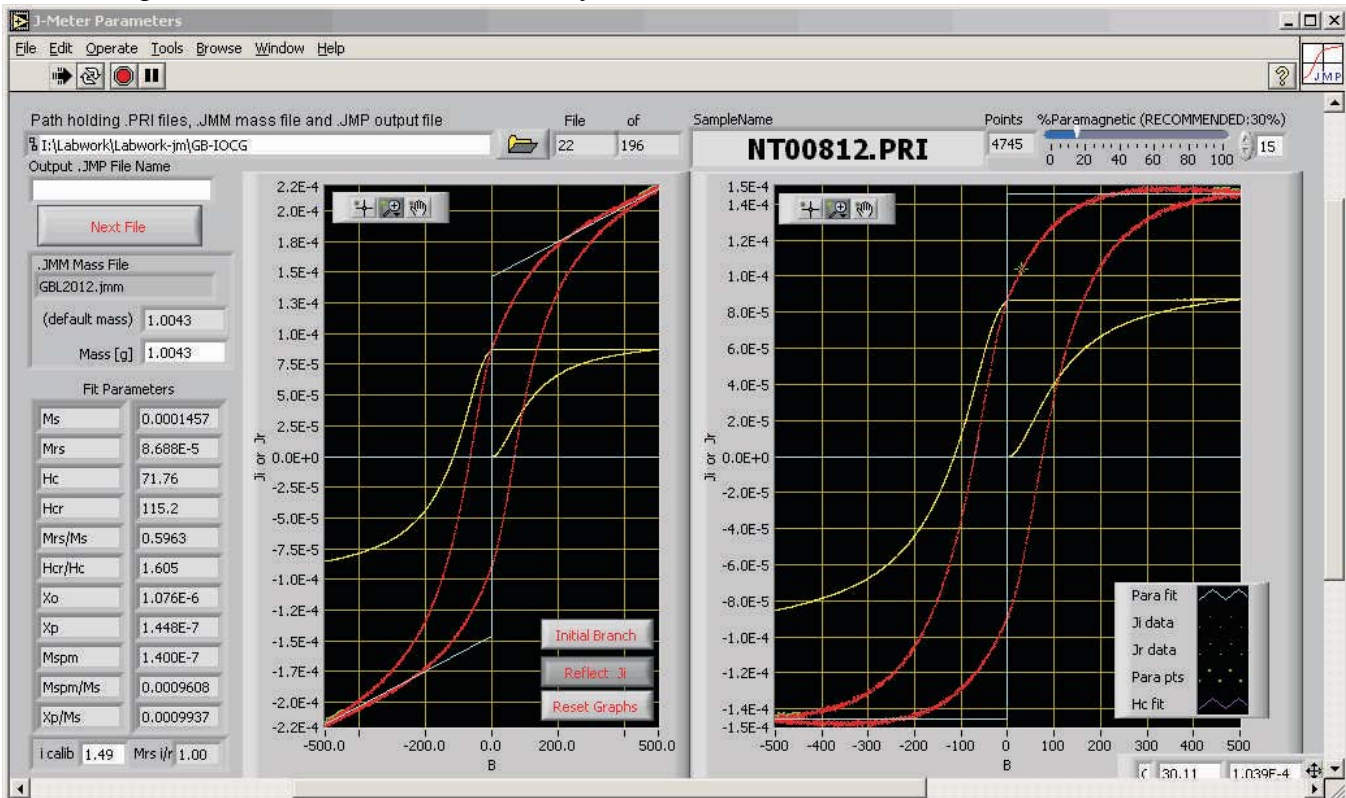
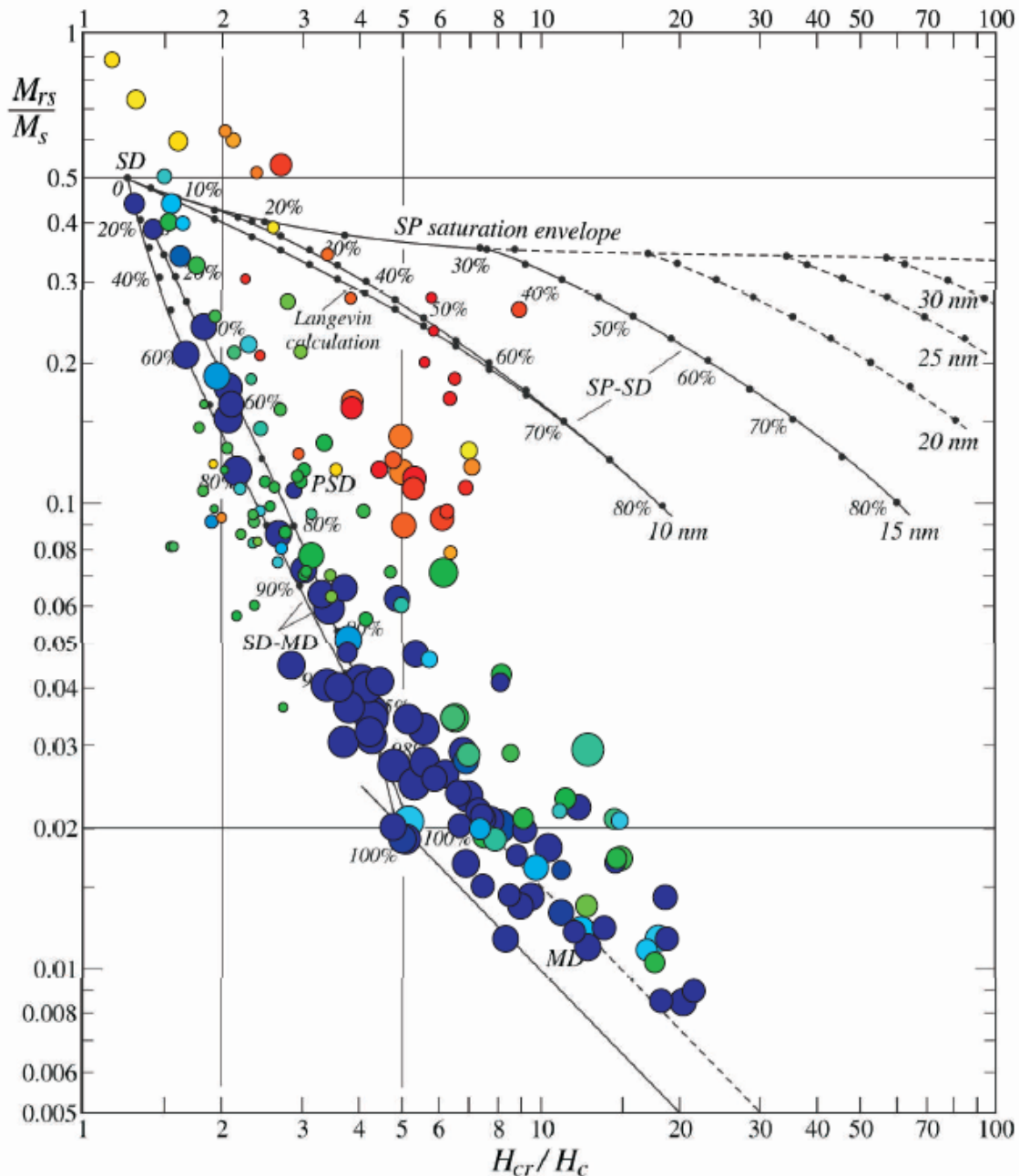


Figure 12: Screen-shot of LabView program JMP to analyze the J-Meter Coercivity Spectrometer output. The red trace marks the induced magnetization and the yellow trace marks the remanent magnetization. The left-hand graph displays the raw measurements, and the right hand graph has the paramagnetic susceptibility (blue lines) removed, revealing the ferromagnetic hysteresis curve.

Dunlop, 2002) which helps specify the magnetic grain sizes in a sample (Fig. 13).

Curie temperatures of the magnetic minerals in a sample are determined by measuring the magnetic susceptibility as a function of temperature with a Bartington MS2WF thermomagnetic susceptibility meter (Fig. 14). Rock chips are placed in a crucible which sits

within a furnace surrounded by a water-cooled susceptibility meter sensor. Magnetic susceptibility is monitored continuously as it is heated up to 700°C. Pyrrhotite is marked by a susceptibility drop between 300°C and 350°C, magnetite with a drop between 550°C and 580°C, and hematite by a drop above 650°C (Fig. 15).



**Figure 13:** The Day plot (biplot of magnetic hysteresis ratios), on a base plot developed by Dunlop (2002) for titanomagnetite, of the Great Bear Iron Oxide Copper Gold (IOCG) database. The distribution displays a wide range of magnetic mineralogy, concentration and grain-size. The point size is proportional to the logarithm of the saturation magnetization ( $M_s$ ). The colour is from degree of high-field saturation, where blue marks complete saturation by 400 mT (typical of magnetite) and the hotter the colour the harder the magnetism. The yellows through reds are typical of hematite.

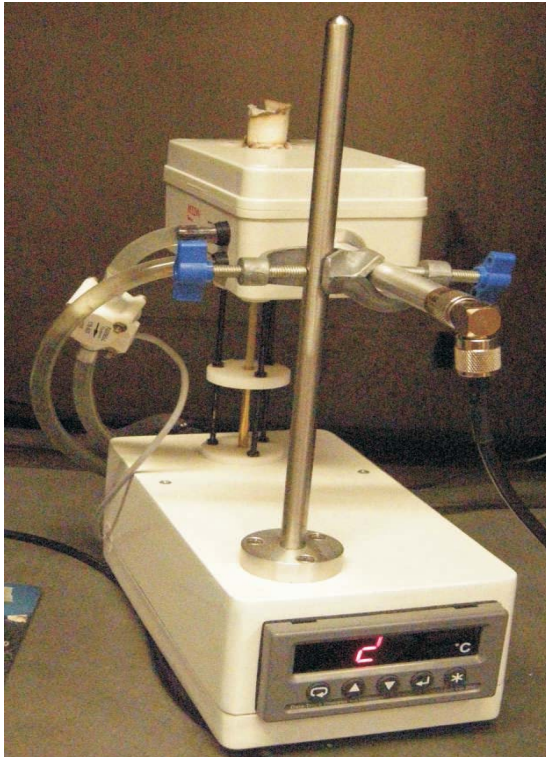


**Figure 14:** Bartington MS2WF Thermomagnetic Susceptibility Meter

Mineral alterations, such as oxidation of sulphides or reduction of hematite to magnetite are also observed during the heating and cooling of the samples. Together with the J-Meter, the Bartington MS2WF produces quantitative measurements of the magnetic mineralogy, grain size and concentration.

## 5. Electrical Properties

Electromagnetic (EM) surveys, including induced polarization (IP) and magnetotelluric (MT) methods, depend on how electric currents traverse through the ground. No physical property of earth materials display as wide a range as electrical resistivity, from native copper and gold around  $10^{-8} \Omega \cdot m$  to quartz around  $10^{14} \Omega \cdot m$ . The critical issue is that the electrical properties are a function not only of the minerals that form the rocks, but also of the fluid pathways that traverse them.

For most rocks, the dominant mode of electrical conductivity is electrolytic conduction through ground water, following Archie's Law

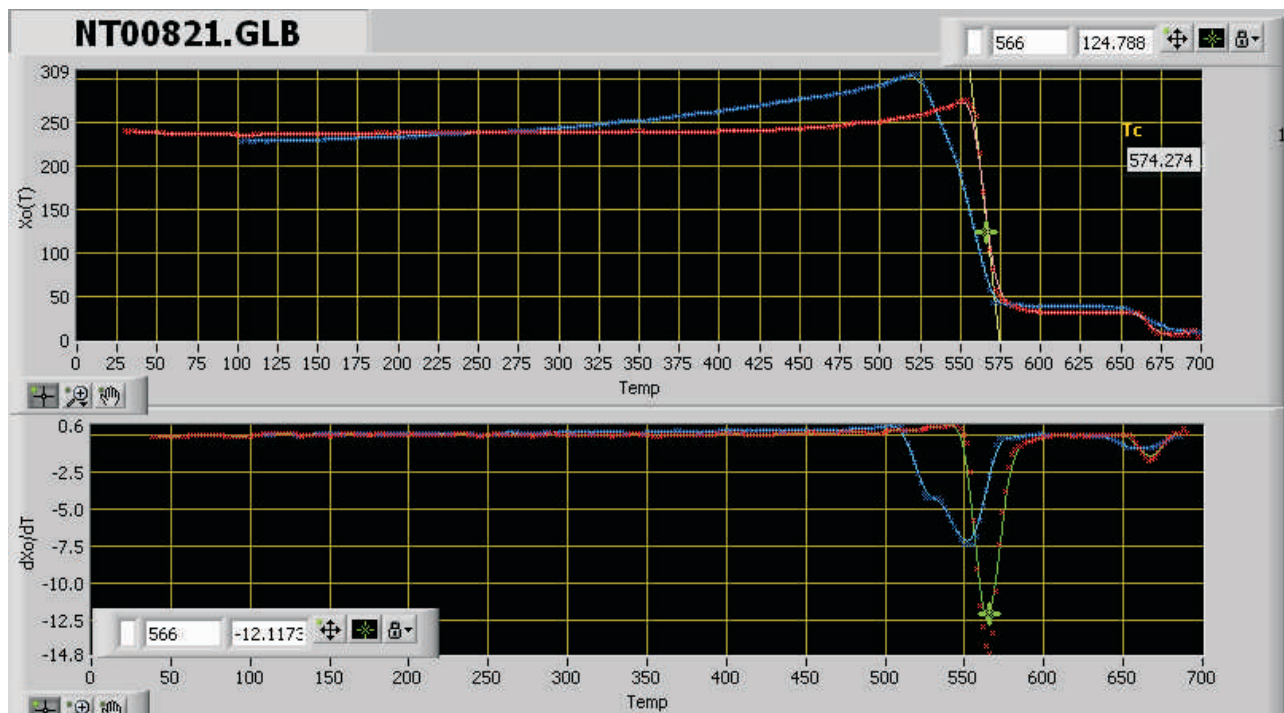


**Figure 15:** Screen-shot of LabView program Xo(T) to analyze Bartington Thermomagnetic Susceptibility Meter output. The top graph shows the magnetic susceptibility as a function of temperature during heating in red and during cooling in blue. The lower graph displays the time derivative of these curves. This sample contains both magnetite, with a Curie temperature of 570°C, and hematite, with a Curie temperature of 670°C.

(Archie, 1942):

$$[\text{eq.7}] \quad \rho = a \varphi^{-m} S_w^{-n} \rho_w,$$

where the resistivity ( $\rho$ ) is proportional to the ground-water resistivity ( $\rho_w$ ), and to other terms describing the rock;  $a$ , a constant depending on rock type; porosity ( $\varphi$ ), the fraction of pore volume containing water ( $S_w$ ); and two empirically determined exponents,  $m$  and  $n$ .

Since there usually is no possibility of recovering the ground water with the rock samples, we approximate the original ground water through vacuum impregnation of the

samples (Fig. 3) with distilled water (conductivity =  $1.6 \times 10^{-4}$  S/m) and let them sit for 24 to 36 hours. During this time, solutes, precipitated on pore walls when the sample originally dried, are dissolved into the water. Our measurements show that the resistivity of the water in the beaker reduces for days and weeks. However, the resistivity of the sample is close to stabilized after about 24 hours (Fig. 16). The interpretation is that the dissolution of the solutes within the pore spaces happens over hours, however, the diffusion of the solutes out of the sample is much slower.

Following vacuum impregnation and all the

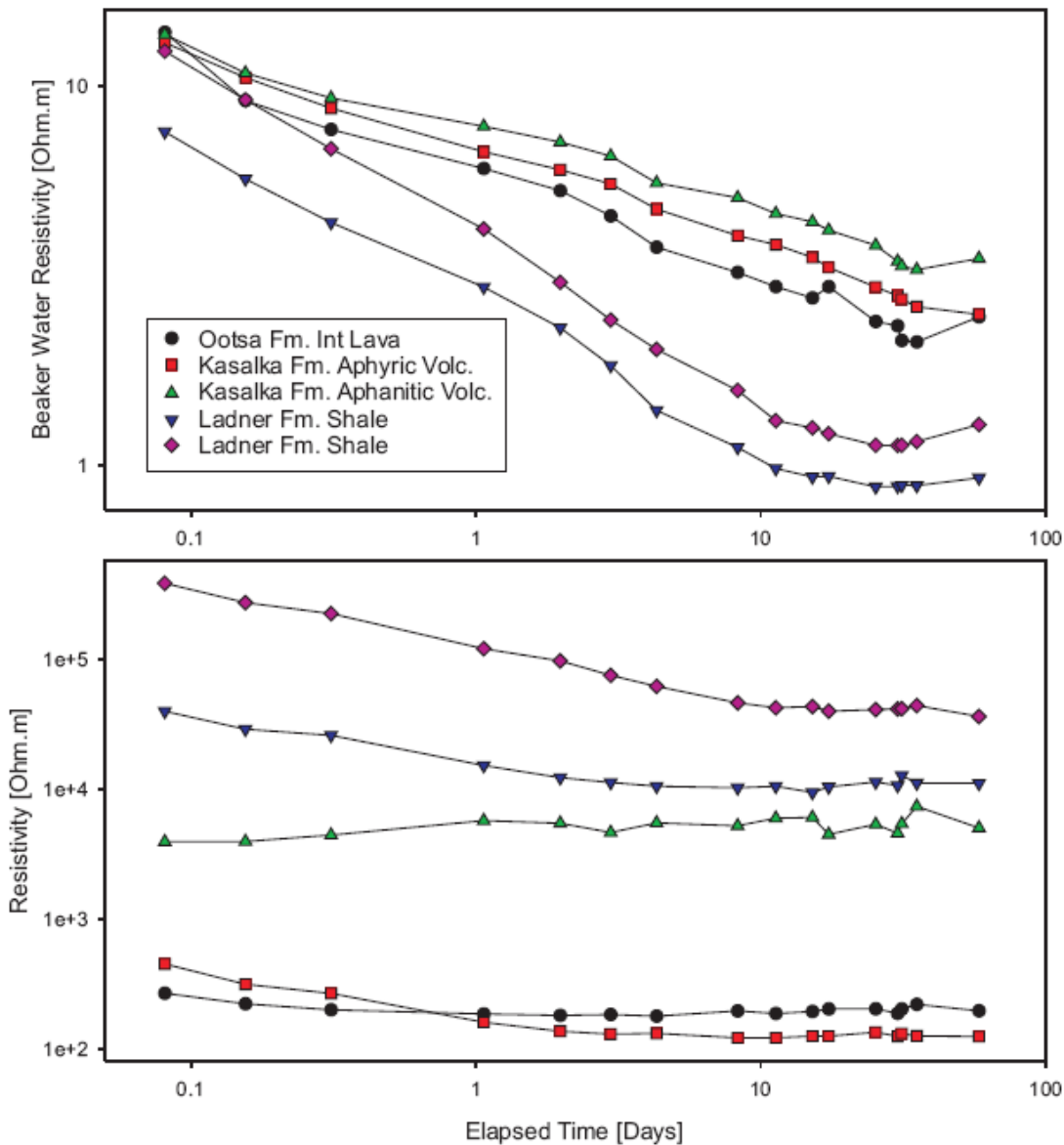


**Figure 16:** The time evolution of the resistivity of 5 rock samples and their immersion water. While the rock resistivity (bottom) usually stabilizes within a day or two, solutes continue to leach into the water for weeks.



weighing procedures necessary for the density and porosity measurements (see Section 3, above), the cylindrical sample is patted dry with a KimWipe<sup>®</sup>. The sample is placed in a sandwich consisting of a large steel washer, a 2 mm thick graphite disk, then the sample, a second graphite disk and finally a second washer (Fig. 17). Using graphite as the contact avoids the problem of free charges accumulating on the contact surfaces. The sample sandwich is placed in a metal box which acts as a Faraday cage, shielding the circuit from high frequency EM waves.

Electrical impedance is a complex quantity; the real component of impedance is a measure of resistance or energy loss in a circuit, and the imaginary component of impedance is a measure of energy storage. An electrical impedance spectrum (EIS) is the frequency dependence of the complex impedance of a sample. The magnitude of the impedance is the ratio of the amplitude of the voltage drop across a sample and the current going through it. Its phase is the phase shift between these two quantities. In the PPL, we use a Solartron 1260 Frequency Response Analyzer to measure the impedance spectrum (Fig. 18). The metal contacts are attached to the current and voltage inputs through grounded coaxial cables. The current is driven with a 1 V sinusoidal wave, at frequencies from 1 MHz down to 0.025 Hz (40 s period) at 5 frequencies each

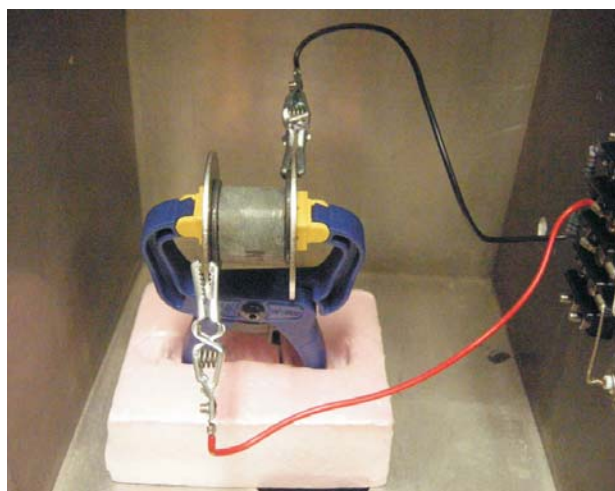


**Figure 17:** Electrode connections for rock electrical impedance measurements. The sample is placed in a sandwich consisting of a large steel washer, a 2 mm thick graphite disk, then the sample, a second graphite disk and finally a second washer.

decade. Above 1 MHz, the sample has little influence on the spectrum while the effects of inductance and standing waves in the probes dominate. At very low frequencies, the dominant control is electrolyte diffusion across the electrode contacts.

The absolute value of the observed resistivity can vary by up to 50 % depending on the state of the water impregnation and the clamping pressure of the sample sandwich. This uncertainty is insignificant as natural resistivities vary over many orders of magnitude and are plotted on logarithmic scales.

New software (ZARCFIT using LabView, Fig. 19) has been developed to model the electrical impedance spectrum in terms of equivalent circuits. The data is presented as both a Cole-Cole plot of the real and imaginary components of the impedance at each frequency (Cole and Cole, 1941), and as Bode plots of the impedance magnitude and phase as a function of frequency. The circuit response, with parameters set with a series of 15 sliders, is also plotted. Once a sufficiently close fit is made by hand, a simplex optimization algorithm minimizes a mismatch function (sum of square deviations) to determine best fit parameters.

Full documentation on how to operate and interpret the program is available from the PPL.



**Figure 18:** Solartron 1260 Frequency Response Analyzer set up to measure rock electrical impedance spectrum.

Here are some important features:

1) The building blocks of the electrical impedance spectrum are “Zarcs”, consisting of a parallel resistor and a constant phase element (Fig. 20). A constant phase element is a modified capacitor. A capacitor has the frequency response:

$$[eq.8] \quad Z_C = 1 / C i \omega ,$$

where  $C$  is the capacitance,  $\omega$  is the angular frequency ( $\omega = 2\pi f$ ) and  $f$  is the linear frequency. The constant phase element has the frequency response:

$$[eq.9] \quad Z_{CPE} = 1 / Q(i\omega)^p ,$$

where  $p$  is an exponent and  $Q$  is the size of the constant phase element. If  $p=1$ , then  $Z_{CPE} = Z_C$  (a capacitor). If  $p=0$ , then  $Z_{CPE} = R$  (a resistor). A Zarc on a Cole-Cole plot has the form of a sector of a circular arc with width equal to the resistance, and with a maximum at angular frequency

$$[eq.10] \quad \omega_0 = (RQ)^{-1/p} .$$

The exponent  $p$  describes the spread in the relaxation times for the circuit element. If  $p=1$ , then the circuit has a single relaxation time  $1/\omega_0$ . The standard deviation of a log-normal distribution of relaxation times increases as  $p$  gets lower.

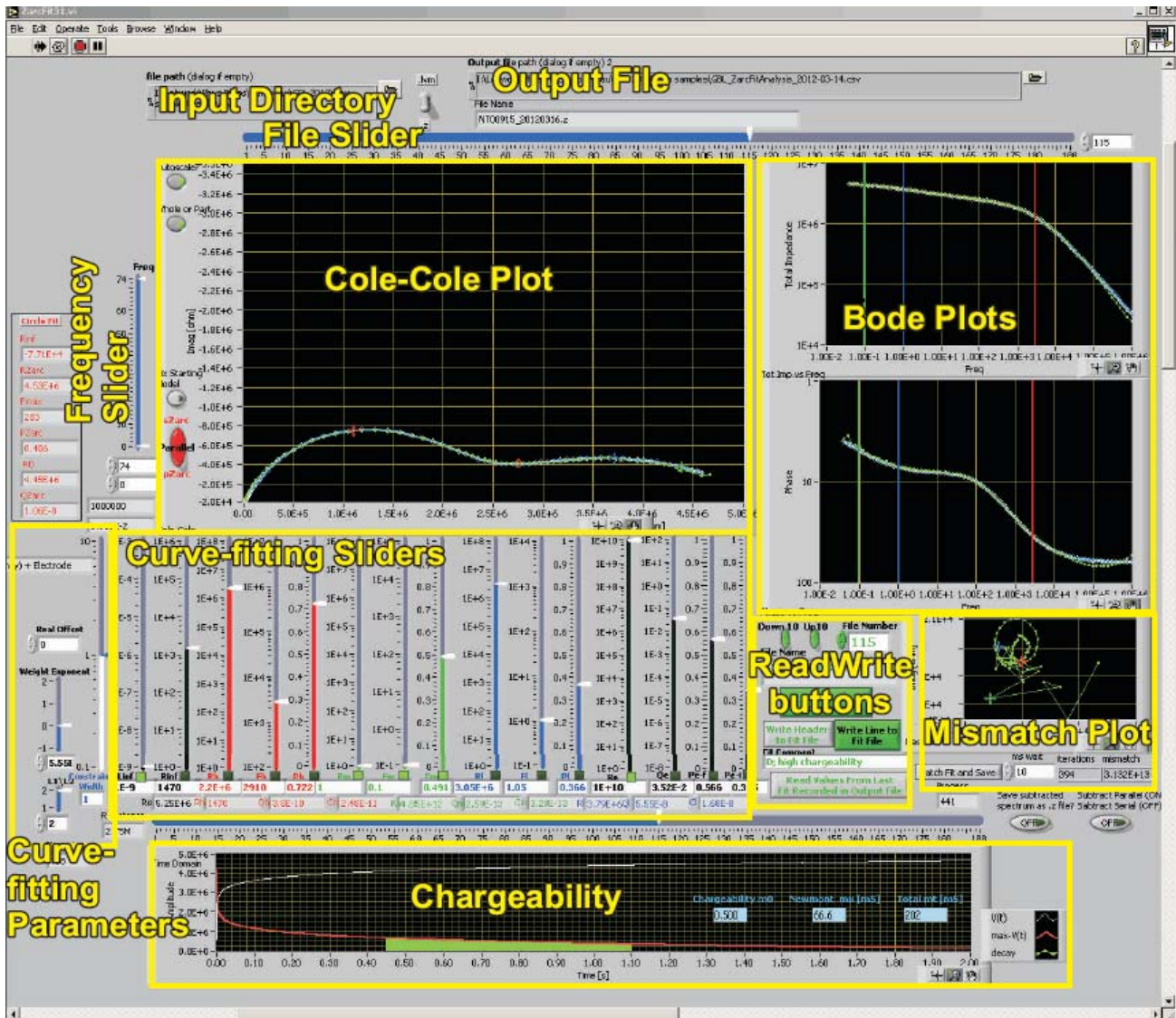
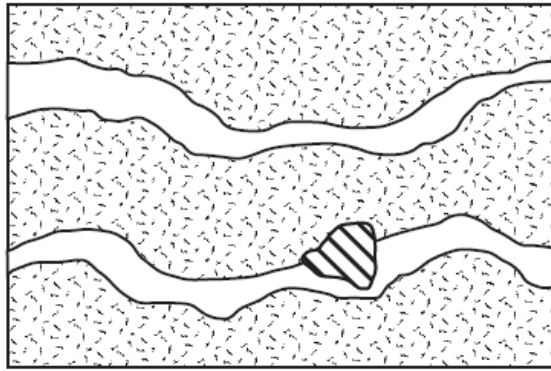
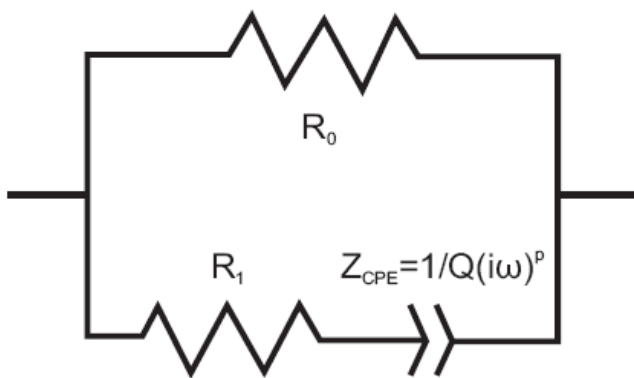


Figure 19: Screenshot of LabView program ZARCFIT for analysis of electrical impedance spectra. The green area in the bottom rectangle is the integration of the time-domain response for chargeability calculation.



Mineralized Rock



Equivalent Circuit

2) The EIS of most rocks are described as a

**Figure 20:** Pelton et al. (1978) model of a mineralized rock and its equivalent electric circuit as a “Zarc”.

single high frequency Zarc, describing the Archie’s law resistance and capacitance derived from the dielectric constant of the sample. We suspect for high resistivity rocks, the observed capacitance arises from the geometry of the apparatus.

3) A low frequency Zarc response is common in rocks (Pelton et al., 1978), especially in weakly mineralized samples (Fig. 20). The mechanism is storage of charge on the surfaces of electrically conductive grains (the electrode effect). This is the response being searched for using induced polarization (IP) techniques.

Time-domain IP report survey results in terms of chargeability, which can be derived from the EIS equivalent circuit determined using ZARCFIT. In an IP survey, electrical current is injected into the ground as a slow square-wave

function. When the current is switched off, the voltage response is a decaying curve. Using the Newmont Standard, the chargeability ( $M_X$ ) is the area under the voltage curve from 430 to 1100 ms, normalized by the beginning voltage (units ms). In ZARCFIT, the sample’s frequency response is converted into time domain by inverse Fourier transform and then numerically integrated (bottom of Fig. 19). An alternative definition, called initial chargeability ( $M_0$ ), is usually defined as the instantaneous drop in voltage after the current is removed. In practical applications, current can never be stopped as a perfect step function, so the drop is measured at some short time after the current was shut down. There is high frequency – short duration storage of charge, as seen by the Archie’s law Zarc, but it is too fast to be observed in a time domain IP measurement. For the determination of  $M_0$  from the sample electrical impedance spectrum, we set the time for measuring the voltage drop to be 1 ms.

4) In series with the rock’s equivalent circuit is the impedance of the apparatus, which must be fit and subtracted from the rock response before the resistance and chargeability are calculated. The apparatus effects are particularly observed at high and low frequencies. In theory, the resistance of the rock ( $R_0$ ) should be the real impedance measured at zero frequency (direct current). Some labs choose the resistance at some arbitrary frequency, whereas others choose the resistance with the minimum phases shift in a frequency range. With ZARCFIT, the apparatus and the rock impedance are simultaneously fit, allowing the rock spectrum to be reliably distinguished and separated. Note that the extrinsic property of resistance is converted to the intrinsic property of resistivity by multiplying the sample resistance by the cross section area ( $A$ ) and divide it by its length ( $l$ ). The ratio  $A/l$  is called the geometric factor.

6) At high frequency ( $>100$  kHz), and only observed in low resistivity rocks ( $R_0 < 10$  k $\Omega$ ), the inductance of the probe wires is seen as the impedance having positive imaginary values and positive phase shifts (i.e., inductance). This effect is modeled with a series inductor:

$$[\text{eq.12}] \quad Z_L = Li\omega,$$

At low frequency, there is the effect of diffusion across the electrodes. Theoretically, this type of impedance should have the form of a Warburg impedance:

$$[eq.13] \quad Z_W = 1 / Q(i\omega)^{1/2}.$$

Empirically we find the low frequency electrode impedance is best described as a modified constant phase element:

$$[eq.14] \quad Z_E = 1 / (Q_E i^{p_i} \omega^{p_f}),$$

where  $p_i$  and  $p_f$  are separate exponents for the phase angle and the frequency. It is important that the electrode EIS be as accurately fit as possible, as it is extrapolated up to frequencies important for the determination of induced polarization chargeability.

7) Rocks naturally provide parallel conduction mechanisms, however the parameters which control a parallel circuit are non-intuitive (Fig. 21). Thus the sliders control the parameters for an equivalent series circuit. The more realistic parallel circuit is used internally for the parameter

optimization and for the interpretation of the petrophysical properties.

With reference to the series and parallel circuits of Figure 21, the following equations are used to transform the intuitive series circuit parameters (un-primed) to the more realistic parallel circuit parameters (with primes). The equations are approximate and are accurate only when there is no significant overlap in the relaxation time ranges between the parallel conduction mechanisms.

$$[eq.15] \quad R'_0 = R_\infty + R_H + R_M + R_L.$$

$$[eq.16] \quad R'_H = R_\infty (R_\infty + R_H) / R_H.$$

$$[eq.17] \quad Q'_H = Q_H (R_H / (R_\infty + R_H))^2.$$

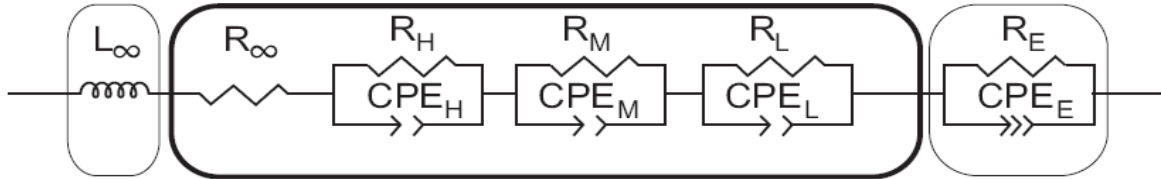
$$[eq.18] \quad R'_M = (R_\infty + R_H) (R_\infty + R_H + R_M) / R_M.$$

$$[eq.19] \quad Q'_M = Q_M (R_M / (R_\infty + R_H + R_M))^2.$$

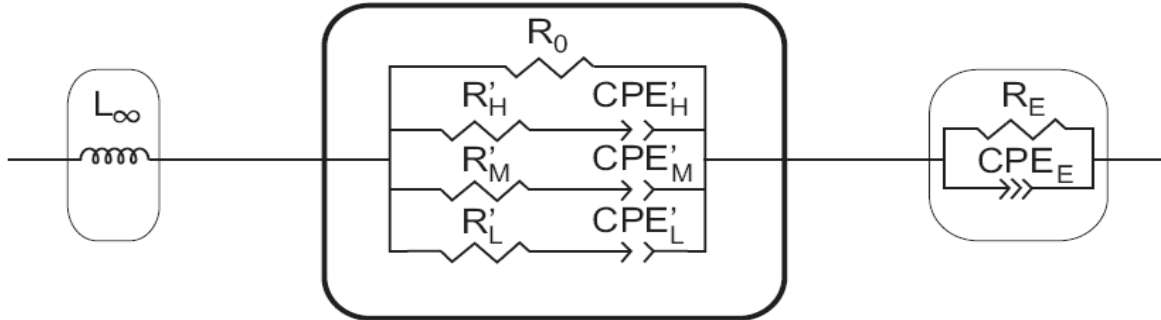
$$[eq.20] \quad R'_L = (R_\infty + R_H + R_M) (R_\infty + R_H + R_M + R_L) / R_L.$$

$$[eq.21] \quad Q'_L = Q_M (R_L / (R_\infty + R_H + R_M + R_L))^2.$$

### Series Circuit, for intuitive manipulation



### Parallel Circuit, more realistic representation



Cables

Rock Sample

Electrodes

**Figure 21:** Equivalent circuits for analyzing rock impedance, including their measurement connections. The series circuit (top) is easier to manipulate, while the parallel circuit (bottom) is more realistic. Thus, the operator works with the analysis as if the equivalent circuit were in series form, while the program does calculations using the equivalent parallel form.

In practice, electrical impedance spectra are fit by manipulating the sliders to produce an approximate fit of the model to the observations, while ensuring that the 15 parameters are realistic. There are many local minima which the optimization procedure could locate, however most are nonsensical. It takes good physics understanding and experience to produce useful fits to the electrical impedance spectra.

Analysis of the electrical impedance spectra, and their relationships to lithology and complementary physical properties measurements, is still in its preliminary phase at the PPL. In Figure 22, the low electrical resistivity samples are dominantly of high magnetic susceptibility and high density, certainly caused by the concentration of sulphides which have high density, high electrical conductivity, and in the Great Bear Magmatic Zone from which these samples were taken, the mineralization is strongly associated with iron oxides. The

compilation of all samples measured to date (Fig. 23) shows that there is an unexpected strong concentration with a mode at 25 kΩ.m, and no clear correlation with chargeability. Note that the low resistivity-high chargeability samples will have the dominant effect on induced polarization surveys.

In summary, a new method has been developed to analyze electrical impedance spectra of rock samples. The program ZARCFIT fits the EIS of the rock and the apparatus together with few assumptions. Although the individual parameters have significance concerning the mineralogy and permeability geometry of the sample, the main important parameters, resistivity and chargeability, are determined and compiled in the rock property database.

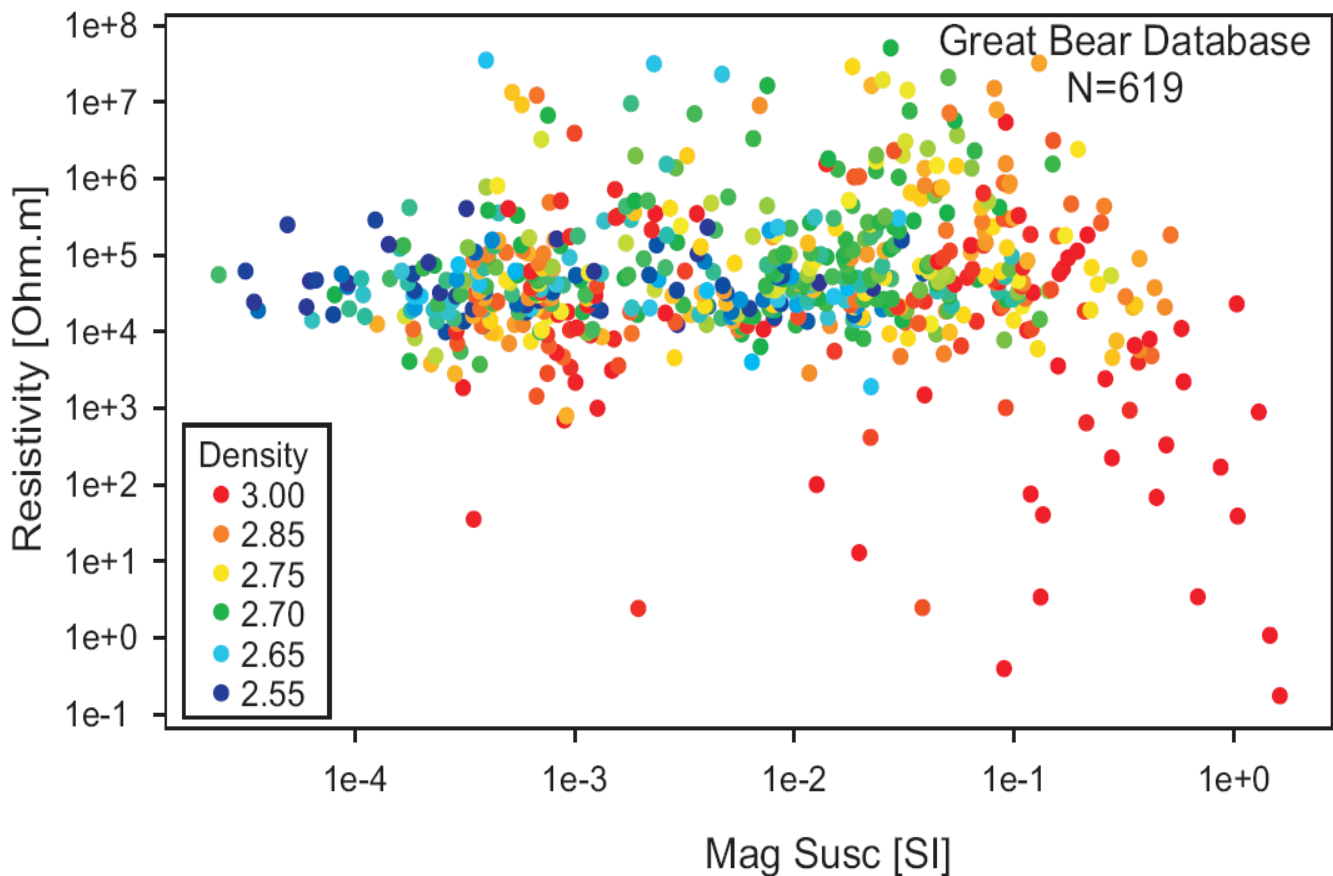


**Figure 22:** Relationship between magnetic susceptibility, density and electrical resistivity in the Great Bear-IOCG database.

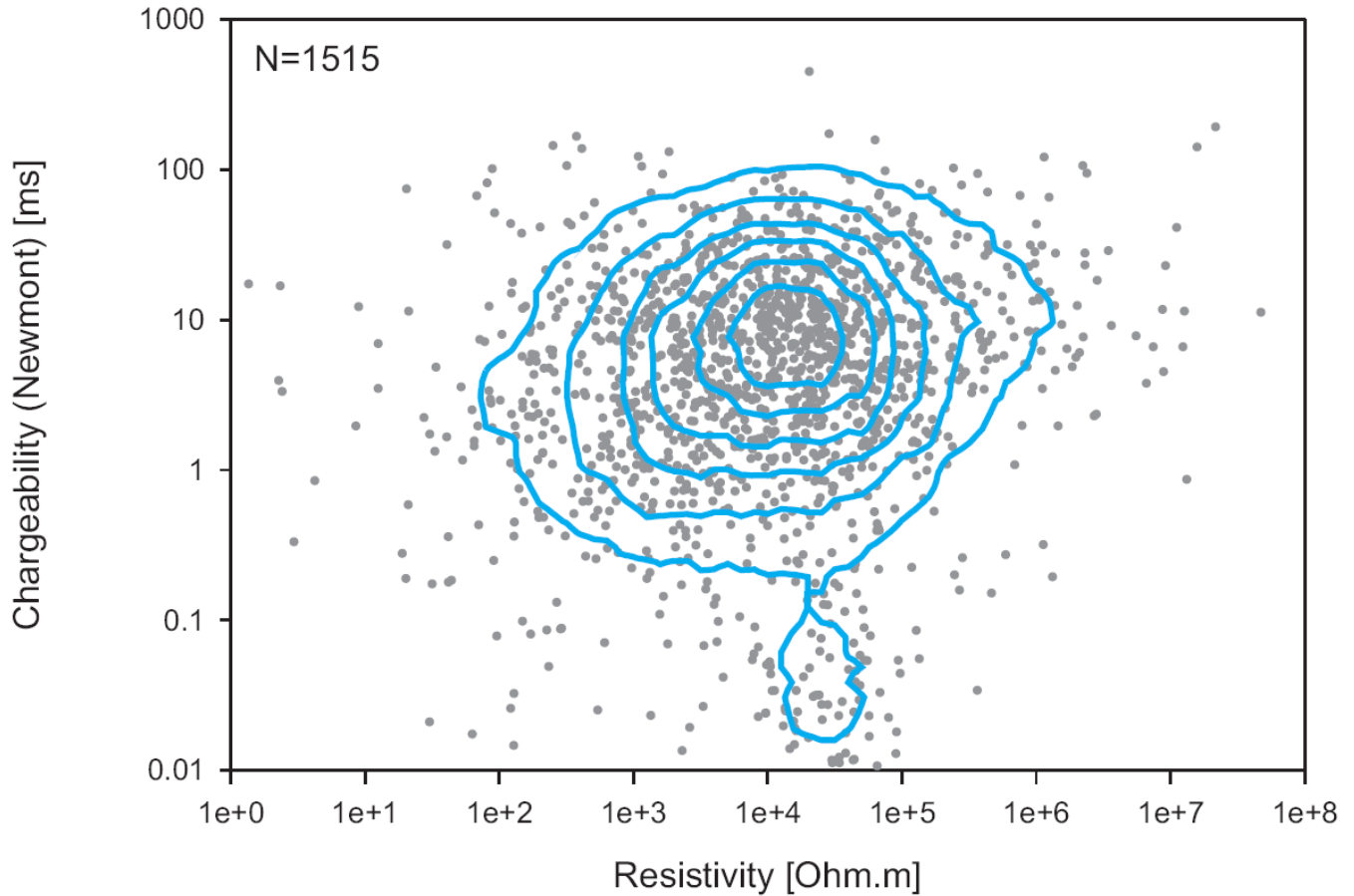


**Figure 23:** Electrical resistivity – chargeability biplot of the British Columbia and Great Bear-IOCG database.

## 6. Summary

The Paleomagnetism and Petrophysics Laboratory (PPL) at the Geophysical Survey of Canada has developed a standard set of measurements of physical properties of rocks. Rock property tables only provide the final results of density, magnetic properties and electrical properties. It is important for geologists and geophysicists who apply these data to understand the methods used, their precision and their limits of applicability. This paper is designed as a single-reference documentation to simplify reporting and application of the rock properties database.

## References

- Archie, G.E., 1942. The electrical resistivity log as an aid in determining some reservoir characteristics; *Petroleum Transactions of AIME*, v. 146, p. 54–62.
- Cole, K.S., and Cole, R.H., 1941. Dispersion and absorption in dielectrics - I Alternating current characteristics". *Journal of Chemical Physics*, v. 9, p. 341–352.
- Day, R., Fuller, M., and Schmidt, V.A., 1977. Hysteresis properties of titanomagnetites: Grain size and composition dependence; *Physics of the Earth and Planetary Interiors*, v. 13, p. 260–267.
- Dunlop, D.J., 2002. Theory and application of the Day plot (Mrs/Ms versus Hcr/Hc) 1. Theoretical curves and tests using titanomagnetite data, *Journal of Geophysical Research*, v. 107, 2056, 22 p., doi:10.1029/2001JB000486.
- Enkin, R.J., Baker, J., Nourgaliev, D., Iassonov, P., and Hamilton, T.S., 2007. Magnetic hysteresis parameters and Dayplot analysis to characterize diagenetic alteration in gas hydrate bearing sediments, *Journal of Geophysical Research*, v. 112, B06S90, doi:10.1029/2006JB004638.
- Enkin, R.J., Vidal, B.S., Baker, J. and Struyk, N.M., 2008. Physical properties and paleomagnetic database for south-central British Columbia; in *Geological Fieldwork 2007*, B.C. Ministry of Energy Mines and Petroleum Resources, Paper 2008-1, p. 5-8.
- Heider, F., Zitzelsberger, A., and Fabian, K., 1996. Magnetic susceptibility and remanent coercive force in grown magnetite crystals from 0.1/xm to 6 mm; *Physics of the Earth and Planetary Interiors*, v. 93, p. 239-256.
- Henkel, H., 1991. Petrophysical properties (density and magnetization) of rocks from the northern part of the Baltic Shield; *Tectonophysics*, v. 192, p. 1–19.
- Henkel, H., 1994. Standard diagrams of magnetic properties and density – a tool for understanding magnetic petrology; *Journal of Applied Geophysics*, v. 32, p. 43–53.
- Jolly, P., 1864. Eine Federwage zu exacten Wägungen; *Sitzb. Akad. Wiss. München*, v. 162, p. 166
- Néel, L., 1955. Some theoretical aspects of rock magnetism; *Advances in Physics*, v. 4, no. 14, p. 191–243.
- Parsons, S., McGaughey, J., Mitchinson, D., Phillips, N. and Lane, T.E., 2009. Development and application of a rock property database for British Columbia; in *Geoscience B.C., Summary of Activities 2008*, Geoscience B.C., Report 2009-1, p. 137–144.
- Pelton, S. H., Ward, S. H., Hallof, P. G., Sill, W. R., and Nelson, P. H., 1978. Mineral discrimination and removal of inductive coupling with multifrequency IP; *Geophysics*, v. 43, p. 588-609.
- Shimamura, K, Williams, S P., and Buller, G, 2008. GanFeld user guide: a map-based field data capture system for geologists; *Geological Survey of Canada, Open File Report 5912*; 90 p; doi:10.4095/226214.

Table 1: GSC GanFeld lithological classification scheme (after Shimamura et al., 2008)

LITHGROUP	LITHTYPE	LITHDETAIL
breccia	cement	hydrothermal
breccia	cement hydrothermal	Ca-Fe (HT) alteration
breccia	cement hydrothermal	Ca-Fe (LT) alteration
breccia	cement hydrothermal	Fe alteration
breccia	cement hydrothermal	K alteration
breccia	cement hydrothermal	K-Fe (HT) alteration
breccia	cement hydrothermal	Na alteration
breccia	cement hydrothermal	other
breccia	cement hydrothermal	phyllic
breccia	cement hydrothermal	silicification, quartz
breccia	cement hydrothermal	unknown
breccia	cement volcanic	see mineral assemblage
breccia	fragment	juvenile
breccia	fragment	lithic
breccia	fragment	plutonic
breccia	fragment	sedimentary
breccia	fragment	volcanic
breccia	fragment	volcaniclastic
breccia	fragment hydrothermally altered	Ca-Fe (HT) alteration
breccia	fragment hydrothermally altered	Fe alteration
breccia	fragment hydrothermally altered	K alteration
breccia	fragment hydrothermally altered	Na alteration
breccia	fragment hydrothermally altered	other
breccia	fragment hydrothermally altered	phyllic
breccia	fragment hydrothermally altered	plutonic
breccia	fragment hydrothermally altered	sedimentary
breccia	fragment hydrothermally altered	silicification, quartz
breccia	fragment hydrothermally altered	unknown
breccia	fragment hydrothermally altered	volcanic
breccia	fragment hydrothermally altered	volcaniclastic
breccia	hydrothermal monomict breccia	matrix to clast-supported
breccia	hydrothermal monomict breccia	matrix-supported
breccia	hydrothermal polymict breccia	clast-supported
breccia	hydrothermal polymict breccia	matrix to clast-supported
breccia	hydrothermal polymict breccia	matrix-supported
breccia	matrix hydrothermally altered	other
breccia	monomict breccia	clast-supported
breccia	monomict breccia	matrix to clast-supported
breccia	monomict breccia	matrix-supported
breccia	monomict breccia hydrothermally	clast-supported
breccia	monomict breccia hydrothermally	matrix to clast-supported
breccia	monomict breccia hydrothermally	matrix-supported
breccia	polymict breccia	clast-supported
breccia	polymict breccia	matrix to clast-supported
breccia	polymict breccia	matrix-supported
breccia	polymict breccia hydrothermally	clast-supported



LITHGROUP	LITHTYPE	LITHDETAIL
breccia	polymict breccia hydrothermally	matrix to clast-supported
breccia	polymict breccia hydrothermally	matrix-supported
hydrothermal	breccia (h)	monomict breccia
hydrothermal	breccia (h)	polymict breccia
hydrothermal	breccia filling (h)	breccia filling
hydrothermal	breccia filling (h)	Ca-Fe (HT) alteration
hydrothermal	breccia filling (h)	Fe alteration
hydrothermal	breccia filling (h)	granite
hydrothermal	breccia filling (h)	K alteration
hydrothermal	breccia filling (h)	metasomatic rock
hydrothermal	breccia filling (h)	propylitic
hydrothermal	breccia filling (h)	see mineral assemblage
hydrothermal	breccia filling (h)	siltstone
hydrothermal	breccia filling (h)	Skarn
hydrothermal	fragment (h)	in situ
hydrothermal	fragment (h)	transported
hydrothermal	fragment (h)	unknown
hydrothermal	pervasive	chloritized
hydrothermal	pervasive	goethitized
hydrothermal	pervasive	silicified
hydrothermal	replacement (h)	Ca-Fe (HT) alteration
hydrothermal	replacement (h)	Ca-Fe (LT) alteration
hydrothermal	replacement (h)	carbonates
hydrothermal	replacement (h)	chlorite
hydrothermal	replacement (h)	epidote
hydrothermal	replacement (h)	Fe alteration
hydrothermal	replacement (h)	impregnation
hydrothermal	replacement (h)	impregnation of protolith
hydrothermal	replacement (h)	K alteration
hydrothermal	replacement (h)	K-Fe (HT) alteration
hydrothermal	replacement (h)	K-Fe (LT) alteration
hydrothermal	replacement (h)	Na alteration
hydrothermal	replacement (h)	other
hydrothermal	replacement (h)	phyllic
hydrothermal	replacement (h)	propylitic
hydrothermal	replacement (h)	recrystallisation
hydrothermal	replacement (h)	recrystallisation of protolith
hydrothermal	replacement (h)	see mineral assemblage
hydrothermal	replacement (h)	Si
hydrothermal	replacement (h)	silicification, quartz
hydrothermal	replacement (h)	skarn
hydrothermal	replacement (h)	tourmaline
hydrothermal	replacement (h)	unknown
hydrothermal	replacement veining (h)	Ca-Fe (HT) alteration
hydrothermal	replacement veining (h)	Ca-Fe (LT) alteration
hydrothermal	replacement veining (h)	Fe alteration
hydrothermal	replacement veining (h)	K alteration

LITHGROUP	LITHTYPE	LITHDETAIL
hydrothermal	replacement veining (h)	K-Fe (HT) alteration
hydrothermal	replacement veining (h)	Na alteration
hydrothermal	replacement veining (h)	other
hydrothermal	replacement veining (h)	phyllic
hydrothermal	replacement veining (h)	propylitic
hydrothermal	replacement veining (h)	silicification, quartz
hydrothermal	replacement veining (h)	unknown
hydrothermal	stockwerk	other
hydrothermal	stockwerk	quartz stockwerk
hydrothermal	stockwerk filling (h)	chert silica
hydrothermal	stockwerk filling (h)	see mineral assemblage
hydrothermal	stockwerk filling (h)	vein filling
hydrothermal	tension vein filling (h)	see mineral assemblage
hydrothermal	vein (h)	barite vein
hydrothermal	vein (h)	Ca-Fe (HT) alteration
hydrothermal	vein (h)	Ca-Fe (LT) alteration
hydrothermal	vein (h)	calcite vein
hydrothermal	vein (h)	calcite-quartz vein
hydrothermal	vein (h)	carbonate vein
hydrothermal	vein (h)	carbonate-quartz vein
hydrothermal	vein (h)	chlorite vein
hydrothermal	vein (h)	dolomite vein
hydrothermal	vein (h)	dolomite-quartz vein
hydrothermal	vein (h)	epidote
hydrothermal	vein (h)	epidote vein
hydrothermal	vein (h)	Fe alteration
hydrothermal	vein (h)	K alteration
hydrothermal	vein (h)	K-Fe (HT) alteration
hydrothermal	vein (h)	K-Fe (LT) alteration
hydrothermal	vein (h)	Na alteration
hydrothermal	vein (h)	other
hydrothermal	vein (h)	oxide vein
hydrothermal	vein (h)	propylitic
hydrothermal	vein (h)	quartz vein
hydrothermal	vein (h)	quartz-calcite vein
hydrothermal	vein (h)	quartz-carbonate vein
hydrothermal	vein (h)	quartz-dolomite vein
hydrothermal	vein (h)	see mineral assemblage
hydrothermal	vein (h)	Si
hydrothermal	vein (h)	siderite vein
hydrothermal	vein (h)	sulphate vein
hydrothermal	vein (h)	sulphide vein
hydrothermal	vein (h)	tourmaline
hydrothermal	vein filling (h)	see mineral assemblage
hydrothermal	vein filling (h)	vein filling
hydrothermal	vein replacement (h)	see mineral assemblage
hydrothermal	vein selvage (h)	Ca-Fe (HT) alteration

**Enkin et al.: Physical Property Measurements at the GSC - Table 1**

<b>LITHGROUP</b>	<b>LITHTYPE</b>	<b>LITHDETAIL</b>
hydrothermal	vein selvage (h)	Fe alteration
hydrothermal	vein selvage (h)	K alteration
hydrothermal	vein selvage (h)	Na alteration
hydrothermal	vein selvage (h)	silicification, quartz
hydrothermal	void fill (h)	agate
hydrothermal	void fill (h)	calcite
hydrothermal	void fill (h)	chalcedony
hydrothermal	void fill (h)	dolomite
hydrothermal	void fill (h)	opal
hydrothermal	void fill (h)	other
hydrothermal	void fill (h)	quartz
hydrothermal	void fill (h)	zeolites
metamorphic	general (m)	altered metamorphic rock
metamorphic	general (m)	amphibolite
metamorphic	general (m)	blueschist
metamorphic	general (m)	calcsilicate
metamorphic	general (m)	crystalline magnesite
metamorphic	general (m)	eclogite
metamorphic	general (m)	garnetite
metamorphic	general (m)	granulite
metamorphic	general (m)	greenschist
metamorphic	general (m)	hornfels
metamorphic	general (m)	marble
metamorphic	general (m)	metamorphic rock
metamorphic	general (m)	metasomatic rock
metamorphic	general (m)	phyllite
metamorphic	general (m)	schist
metamorphic	general (m)	serpentinite
metamorphic	general (m)	skarn
metamorphic	general (m)	slate
metamorphic	general (m)	sub-greenschist
metamorphic	general hydrothermally altered (m)	altered metamorphic rock
metamorphic	general hydrothermally altered (m)	amphibolite
metamorphic	general hydrothermally altered (m)	metasomatic rock
metamorphic	general hydrothermally altered (m)	schist
metamorphic	gneisses (m)	gneiss
metamorphic	gneisses (m)	orthogneiss
metamorphic	gneisses (m)	paragneiss
metamorphic	migmatitic (m)	agmatite
metamorphic	migmatitic (m)	diatexite
metamorphic	migmatitic (m)	injection migmatite
metamorphic	migmatitic (m)	leucosome
metamorphic	migmatitic (m)	melanosome
metamorphic	migmatitic (m)	metatexite
metamorphic	migmatitic (m)	migmatite
metamorphic	migmatitic (m)	neosome
metamorphic	retrograde (m)	retrograde amphibolite

**Enkin et al.: Physical Property Measurements at the GSC - Table 1**

<b>LITHGROUP</b>	<b>LITHTYPE</b>	<b>LITHDETAIL</b>
metamorphic	retrograde (m)	retrograde gneiss
metamorphic	retrograde (m)	retrograde granulite
metamorphic	retrograde (m)	retrograde metamorphic rock
metamorphic	retrograde (m)	retrograde schist
metaplutonic	felsic (mp)	alaskite
metaplutonic	felsic (mp)	alkali-feld quartz syenite
metaplutonic	felsic (mp)	alkali-feldspar granite
metaplutonic	felsic (mp)	alkali-feldspar syenite
metaplutonic	felsic (mp)	aplite
metaplutonic	felsic (mp)	charnockite
metaplutonic	felsic (mp)	felsic orthogneiss
metaplutonic	felsic (mp)	granite
metaplutonic	felsic (mp)	granitic pegmatite
metaplutonic	felsic (mp)	granodiorite
metaplutonic	felsic (mp)	mangerite
metaplutonic	felsic (mp)	monzodiorite
metaplutonic	felsic (mp)	monzogranite
metaplutonic	felsic (mp)	monzonite
metaplutonic	felsic (mp)	quartz monzonite
metaplutonic	felsic (mp)	quartz syenite
metaplutonic	felsic (mp)	syenite
metaplutonic	felsic (mp)	syenogranite
metaplutonic	felsic (mp)	tonalite
metaplutonic	felsic (mp)	trondhjemite
metaplutonic	intermediate (mp)	diorite
metaplutonic	intermediate (mp)	intermediate orthogneiss
metaplutonic	intermediate (mp)	monzodiorite
metaplutonic	intermediate (mp)	monzogabbro
metaplutonic	intermediate (mp)	quartz diorite
metaplutonic	intermediate (mp)	quartz monzodiorite
metaplutonic	intermediate hydrothermally altered (mp)	diorite
metaplutonic	mafic (mp)	anorthosite
metaplutonic	mafic (mp)	diabase
metaplutonic	mafic (mp)	gabbro
metaplutonic	mafic (mp)	mafic lamprophyre
metaplutonic	mafic (mp)	mafic orthogneiss
metaplutonic	mafic (mp)	mafic pegmatite
metaplutonic	mafic (mp)	metagabbro
metaplutonic	mafic (mp)	norite
metaplutonic	mafic (mp)	troctolite
metaplutonic	silica undersaturated (mp)	essexite
metaplutonic	silica undersaturated (mp)	foid lamprophyre
metaplutonic	silica undersaturated (mp)	foid monzodiorite
metaplutonic	silica undersaturated (mp)	foid monzogabbro
metaplutonic	silica undersaturated (mp)	foid monzosyenite
metaplutonic	silica undersaturated (mp)	foid orthogneiss
metaplutonic	silica undersaturated (mp)	foid syenite

**Enkin et al.: Physical Property Measurements at the GSC - Table 1**

<b>LITHGROUP</b>	<b>LITHTYPE</b>	<b>LITHDETAIL</b>
metaplutonic	silica undersaturated (mp)	foidolite
metaplutonic	ultramafic (mp)	carbonatite
metaplutonic	ultramafic (mp)	clinopyroxenite
metaplutonic	ultramafic (mp)	dunite
metaplutonic	ultramafic (mp)	harzburgite
metaplutonic	ultramafic (mp)	hornblende clinopyroxenite
metaplutonic	ultramafic (mp)	hornblendite
metaplutonic	ultramafic (mp)	kimberlite
metaplutonic	ultramafic (mp)	lherzolite
metaplutonic	ultramafic (mp)	metapyroxenite
metaplutonic	ultramafic (mp)	peridotite
metaplutonic	ultramafic (mp)	pyroxenite
metaplutonic	ultramafic (mp)	serpentinite
metaplutonic	ultramafic (mp)	ultramafic lamprophyre
metaplutonic	ultramafic (mp)	ultramafic metavolcanic rock
metaplutonic	ultramafic (mp)	ultramafic orthogneiss
metaplutonic	ultramafic (mp)	ultramafic schist
metasedimentary	carbonate (ms)	aragonite marble
metasedimentary	carbonate (ms)	calcareous schist
metasedimentary	carbonate (ms)	calcite marble
metasedimentary	carbonate (ms)	calcsilicate
metasedimentary	carbonate (ms)	calcsilicate gneiss
metasedimentary	carbonate (ms)	dolomite marble
metasedimentary	carbonate (ms)	marble
metasedimentary	carbonate (ms)	metasandstone
metasedimentary	carbonate (ms)	skarn
metasedimentary	carbonate hydrothermally altered (ms)	calcareous schist
metasedimentary	carbonate hydrothermally altered (ms)	calcsilicate
metasedimentary	carbonate hydrothermally altered (ms)	calcsilicate gneiss
metasedimentary	carbonate hydrothermally altered (ms)	marble
metasedimentary	carbonate hydrothermally altered (ms)	skarn
metasedimentary	ironstone (ms)	banded iron formation
metasedimentary	siliciclastic (ms)	argillite
metasedimentary	siliciclastic (ms)	garnetite
metasedimentary	siliciclastic (ms)	metachert
metasedimentary	siliciclastic (ms)	metaconglomerate
metasedimentary	siliciclastic (ms)	metaironstone
metasedimentary	siliciclastic (ms)	metaquartzite
metasedimentary	siliciclastic (ms)	metasandstone
metasedimentary	siliciclastic (ms)	metasedimentary granulite
metasedimentary	siliciclastic (ms)	metasiltstone
metasedimentary	siliciclastic (ms)	mica schist
metasedimentary	siliciclastic (ms)	paragneiss
metasedimentary	siliciclastic (ms)	pelite
metasedimentary	siliciclastic (ms)	pelitic gneiss
metasedimentary	siliciclastic (ms)	pelitic granulite
metasedimentary	siliciclastic (ms)	pelitic hornfels

**Enkin et al.: Physical Property Measurements at the GSC - Table 1**

<b>LITHGROUP</b>	<b>LITHTYPE</b>	<b>LITHDETAIL</b>
metasedimentary	siliciclastic (ms)	pelitic schist
metasedimentary	siliciclastic (ms)	phyllite
metasedimentary	siliciclastic (ms)	phyllitic argillite
metasedimentary	siliciclastic (ms)	psammite
metasedimentary	siliciclastic (ms)	psammitic gneiss
metasedimentary	siliciclastic (ms)	psammitic schist
metasedimentary	siliciclastic (ms)	semi-pelite
metasedimentary	siliciclastic (ms)	semi-pelitic granulite
metasedimentary	siliciclastic (ms)	semi-pelitic hornfels
metasedimentary	siliciclastic (ms)	semi-pelitic schist
metasedimentary	siliciclastic (ms)	slate
metasedimentary	siliciclastic hydrothermally altered (ms)	metachert
metasedimentary	siliciclastic hydrothermally altered (ms)	metaironstone
metasedimentary	siliciclastic hydrothermally altered (ms)	metaquartzite
metasedimentary	siliciclastic hydrothermally altered (ms)	metasandstone
metasedimentary	siliciclastic hydrothermally altered (ms)	metasiltstone
metasedimentary	siliciclastic hydrothermally altered (ms)	paragneiss
metavolcanic	bombs (vc)	basalt
metavolcanic	felsic (mv)	alkali-feld quartz trachyte
metavolcanic	felsic (mv)	alkali-feldspar rhyolite
metavolcanic	felsic (mv)	alkali-feldspar trachyte
metavolcanic	felsic (mv)	comendite
metavolcanic	felsic (mv)	dacite
metavolcanic	felsic (mv)	felsic metavolcanic rock
metavolcanic	felsic (mv)	felsic volcanic rock
metavolcanic	felsic (mv)	felsite
metavolcanic	felsic (mv)	pantellerite
metavolcanic	felsic (mv)	pumice
metavolcanic	felsic (mv)	quartz latite
metavolcanic	felsic (mv)	quartz trachyte
metavolcanic	felsic (mv)	rhyodacite
metavolcanic	felsic (mv)	rhyolite
metavolcanic	felsic (mv)	trachyte
metavolcanic	intermediate (mv)	andesite
metavolcanic	intermediate (mv)	basaltic andesite
metavolcanic	intermediate (mv)	boninite
metavolcanic	intermediate (mv)	diabase
metavolcanic	intermediate (mv)	intermed metavolcanic rock
metavolcanic	intermediate (mv)	intermediate volcanic rock
metavolcanic	intermediate (mv)	latite
metavolcanic	intermediate (mv)	quartz andesite
metavolcanic	intermediate (mv)	trachyandesite
metavolcanic	mafic (mv)	amphibolite
metavolcanic	mafic (mv)	amphibolite schist
metavolcanic	mafic (mv)	basalt
metavolcanic	mafic (mv)	greenstone
metavolcanic	mafic (mv)	komatiitic basalt

**Enkin et al.: Physical Property Measurements at the GSC - Table 1**

<b>LITHGROUP</b>	<b>LITHTYPE</b>	<b>LITHDETAIL</b>
metavolcanic	mafic (mv)	mafic metavolcanic rock
metavolcanic	mafic (mv)	mafic volcanic rock
metavolcanic	mafic (mv)	metabasalt
metavolcanic	mafic (mv)	metabasite
metavolcanic	mafic (mv)	obsidian
metavolcanic	mafic (mv)	trachybasalt
metavolcanic	porphyry (mv)	feldspar porphyry
metavolcanic	porphyry (mv)	feldspar-quartz porphyry
metavolcanic	silica undersaturated (mv)	basanite
metavolcanic	silica undersaturated (mv)	foiid metavolcanic rock
metavolcanic	silica undersaturated (mv)	foidite
metavolcanic	silica undersaturated (mv)	nephelinite
metavolcanic	silica undersaturated (mv)	phonolite
metavolcanic	silica undersaturated (mv)	tephrite
metavolcanic	ultramafic (mv)	komatiite
metavolcanic	ultramafic (mv)	picrite
metavolcanic	ultramafic (mv)	serpentinite
metavolcanic	ultramafic (mv)	ultramafic lamprophyre
metavolcanic	ultramafic (mv)	ultramafic metavolcanic rock
metavolcanic	ultramafic (mv)	ultramafic schist
metavolcanic	ultramafic (mv)	ultramafic volcanic rock
metavolcaniclastic	ash (mvc)	ash flow
metavolcaniclastic	ash (mvc)	bentonite
metavolcaniclastic	ash (mvc)	felsic ash tuff
metavolcaniclastic	ash (mvc)	felsic tuff
metavolcaniclastic	ash (mvc)	foiid ash tuff
metavolcaniclastic	ash (mvc)	foiid tuff
metavolcaniclastic	ash (mvc)	intermediate ash tuff
metavolcaniclastic	ash (mvc)	intermediate tuff
metavolcaniclastic	ash (mvc)	mafic ash tuff
metavolcaniclastic	ash (mvc)	mafic tuff
metavolcaniclastic	ash (mvc)	pumice
metavolcaniclastic	ash (mvc)	ultramafic ash tuff
metavolcaniclastic	ash (mvc)	ultramafic tuff
metavolcaniclastic	bombs (mvc)	felsic agglomerate
metavolcaniclastic	bombs (mvc)	foiid agglomerate
metavolcaniclastic	bombs (mvc)	intermediate agglomerate
metavolcaniclastic	bombs (mvc)	mafic agglomerate
metavolcaniclastic	bombs (mvc)	scoria
metavolcaniclastic	bombs (mvc)	ultramafic agglomerate
metavolcaniclastic	breccia (mvc)	felsic pyroclastic breccia
metavolcaniclastic	breccia (mvc)	felsic tuff breccia
metavolcaniclastic	breccia (mvc)	felsic volcanic breccia
metavolcaniclastic	breccia (mvc)	foiid pyroclastic breccia
metavolcaniclastic	breccia (mvc)	foiid tuff breccia
metavolcaniclastic	breccia (mvc)	foiid volcanic breccia
metavolcaniclastic	breccia (mvc)	intermed pyroclastic breccia

**Enkin et al.: Physical Property Measurements at the GSC - Table 1**

<b>LITHGROUP</b>	<b>LITHTYPE</b>	<b>LITHDETAIL</b>
metavolcaniclastic	breccia (mvc)	intermediate tuff breccia
metavolcaniclastic	breccia (mvc)	intermediate volcanic breccia
metavolcaniclastic	breccia (mvc)	mafic pyroclastic breccia
metavolcaniclastic	breccia (mvc)	mafic tuff breccia
metavolcaniclastic	breccia (mvc)	mafic volcanic breccia
metavolcaniclastic	breccia (mvc)	ultramaf pyroclastic breccia
metavolcaniclastic	breccia (mvc)	ultramafic tuff breccia
metavolcaniclastic	breccia (mvc)	ultramafic volcanic breccia
metavolcaniclastic	breccia (mvc)	volcanic breccia
metavolcaniclastic	intermediate (mvc)	intermediate lapilli tuff
metavolcaniclastic	lapilli (mvc)	felsic lapilli stone
metavolcaniclastic	lapilli (mvc)	felsic lapilli tuff
metavolcaniclastic	lapilli (mvc)	foiid lapilli stone
metavolcaniclastic	lapilli (mvc)	foiid lapilli tuff
metavolcaniclastic	lapilli (mvc)	intermediate lapilli stone
metavolcaniclastic	lapilli (mvc)	intermediate lapilli tuff
metavolcaniclastic	lapilli (mvc)	mafic lapilli stone
metavolcaniclastic	lapilli (mvc)	mafic lapilli tuff
metavolcaniclastic	lapilli (mvc)	ultramafic lapilli stone
metavolcaniclastic	lapilli (mvc)	ultramafic lapilli tuff
metavolcaniclastic	volcanic sedimentary (mvc)	volcanic conglomerate
metavolcaniclastic	volcanic sedimentary (mvc)	volcanic mudstone
metavolcaniclastic	volcanic sedimentary (mvc)	volcanic sandstone
metavolcaniclastic	volcanic sedimentary (mvc)	volcanic siltstone
metavolcaniclastic	volcanic sedimentary (mvc)	volcaniclastic rock
plutonic	felsic (p)	alaskite
plutonic	felsic (p)	alkali-feld quartz syenite
plutonic	felsic (p)	alkali-feldspar granite
plutonic	felsic (p)	alkali-feldspar syenite
plutonic	felsic (p)	aplite
plutonic	felsic (p)	charnockite
plutonic	felsic (p)	granite
plutonic	felsic (p)	granitic pegmatite
plutonic	felsic (p)	granodiorite
plutonic	felsic (p)	mangerite
plutonic	felsic (p)	monzogranite
plutonic	felsic (p)	monzonite
plutonic	felsic (p)	quartz monzonite
plutonic	felsic (p)	quartz syenite
plutonic	felsic (p)	syenite
plutonic	felsic (p)	syenogranite
plutonic	felsic (p)	tonalite
plutonic	felsic (p)	trondhjemite
plutonic	felsic hydrothermally altered (p)	alkali-feld quartz syenite
plutonic	felsic hydrothermally altered (p)	alkali-feldspar granite
plutonic	felsic hydrothermally altered (p)	aplite
plutonic	felsic hydrothermally altered (p)	granite



LITHGROUP	LITHTYPE	LITHDETAIL
plutonic	felsic hydrothermally altered (p)	granodiorite
plutonic	felsic hydrothermally altered (p)	monzogranite
plutonic	felsic hydrothermally altered (p)	monzonite
plutonic	felsic hydrothermally altered (p)	quartz monzonite
plutonic	felsic hydrothermally altered (p)	syenite
plutonic	felsic hydrothermally altered (p)	tonalite
plutonic	intermediate (p)	diorite
plutonic	intermediate (p)	Hb diorite
plutonic	intermediate (p)	hydrothermally altered
plutonic	intermediate (p)	monzodiorite
plutonic	intermediate (p)	monzogabbro
plutonic	intermediate (p)	quartz diorite
plutonic	intermediate (p)	quartz monzodiorite
plutonic	intermediate hydrothermally altered (p)	diorite
plutonic	mafic (p)	Amphibole-lamprophyre
plutonic	mafic (p)	anorthosite
plutonic	mafic (p)	diabase
plutonic	mafic (p)	gabbro
plutonic	mafic (p)	gabbro-norite
plutonic	mafic (p)	hydrothermally altered
plutonic	mafic (p)	mafic lamprophyre
plutonic	mafic (p)	mafic pegmatite
plutonic	mafic (p)	mica-lamprophyre
plutonic	mafic (p)	micro-diabase
plutonic	mafic (p)	micro-gabbro
plutonic	mafic (p)	norite
plutonic	mafic (p)	olivine gabbro
plutonic	mafic (p)	Ol-Px-lamprophyre
plutonic	mafic (p)	troctolite
plutonic	mafic hydrothermally altered (p)	diabase
plutonic	mafic hydrothermally altered (p)	mafic lamprophyre
plutonic	silica undersaturated (p)	essexite
plutonic	silica undersaturated (p)	foid diorite
plutonic	silica undersaturated (p)	foid gabbro
plutonic	silica undersaturated (p)	foid lamprophyre
plutonic	silica undersaturated (p)	foid monzodiorite
plutonic	silica undersaturated (p)	foid monzogabbro
plutonic	silica undersaturated (p)	foid monzosyenite
plutonic	silica undersaturated (p)	foid syenite
plutonic	silica undersaturated (p)	foidolite
plutonic	ultramafic (p)	carbonatite
plutonic	ultramafic (p)	clinopyroxenite
plutonic	ultramafic (p)	dunite
plutonic	ultramafic (p)	harzburgite
plutonic	ultramafic (p)	hb clinopyroxenite
plutonic	ultramafic (p)	hornblende clinopyroxenite
plutonic	ultramafic (p)	hornblendite

**Enkin et al.: Physical Property Measurements at the GSC - Table 1**

<b>LITHGROUP</b>	<b>LITHTYPE</b>	<b>LITHDETAIL</b>
plutonic	ultramafic (p)	kimberlite
plutonic	ultramafic (p)	lherzolite
plutonic	ultramafic (p)	orthopyroxenite
plutonic	ultramafic (p)	peridotite
plutonic	ultramafic (p)	pyroxenite
plutonic	ultramafic (p)	ultramafic (p)
plutonic	ultramafic (p)	ultramafic lamprophyre
plutonic	ultramafic (p)	websterite
plutonic	ultramafic (p)	wehrlite
sedimentary	breccia (s)	breccia
sedimentary	breccia (s)	diagenetic breccia
sedimentary	breccia (s)	intraclast breccia
sedimentary	breccia (s)	lithoclast breccia
sedimentary	breccia (s)	monomict breccia
sedimentary	breccia (s)	oligomictic breccia
sedimentary	breccia (s)	polymict breccia
sedimentary	breccia (s)	solution-collapse breccia
sedimentary	coal (s)	anthracite
sedimentary	coal (s)	bituminous coal
sedimentary	coal (s)	coal
sedimentary	coal (s)	lignite
sedimentary	coal (s)	sub-bituminous coal
sedimentary	conglomerate (s)	conglomerate
sedimentary	conglomerate (s)	diamictite
sedimentary	conglomerate (s)	flat-pebble conglomerate
sedimentary	conglomerate (s)	intraclast conglomerate
sedimentary	conglomerate (s)	intraformational conglomerate
sedimentary	conglomerate (s)	monomict conglomerate
sedimentary	conglomerate (s)	oligomictic conglomerate
sedimentary	conglomerate (s)	orthoconglomerate
sedimentary	conglomerate (s)	paraconglomerate
sedimentary	conglomerate (s)	petromict conglomerate
sedimentary	conglomerate (s)	polymict conglomerate
sedimentary	dolostone (s)	crystalline dolostone
sedimentary	dolostone (s)	doloarenite
sedimentary	dolostone (s)	dolobafflestone
sedimentary	dolostone (s)	dolobindstone
sedimentary	dolostone (s)	doloboundstone
sedimentary	dolostone (s)	dolofloatstone
sedimentary	dolostone (s)	doloframestone
sedimentary	dolostone (s)	dolograinstone
sedimentary	dolostone (s)	dololutite
sedimentary	dolostone (s)	dolomicrite
sedimentary	dolostone (s)	dolomitized coquina
sedimentary	dolostone (s)	dolomudstone
sedimentary	dolostone (s)	dolopackstone
sedimentary	dolostone (s)	dolorudstone

LITHGROUP	LITHTYPE	LITHDETAIL
sedimentary	dolostone (s)	dolosiltite
sedimentary	dolostone (s)	dolostone
sedimentary	dolostone (s)	dolowackestone
sedimentary	dolostone (s)	stromatolitic dolostone
sedimentary	evaporite (s)	anhydrite
sedimentary	evaporite (s)	bedded gypsum
sedimentary	evaporite (s)	carbonate evaporite
sedimentary	evaporite (s)	evaporite
sedimentary	evaporite (s)	gypsum
sedimentary	evaporite (s)	gypsum-satinspar veins
sedimentary	evaporite (s)	halite
sedimentary	evaporite (s)	nodular gypsum
sedimentary	evaporite (s)	selenite
sedimentary	evaporite (s)	sylvite
sedimentary	fine clastic (s)	clay shale
sedimentary	fine clastic (s)	claystone
sedimentary	fine clastic (s)	mudrock
sedimentary	fine clastic (s)	mudstone
sedimentary	fine clastic (s)	shale
sedimentary	fine clastic (s)	siltstone
sedimentary	fine clastic hydrothermally altered (s)	mudrock
sedimentary	fine clastic hydrothermally altered (s)	shale
sedimentary	fine clastic hydrothermally altered (s)	siltstone
sedimentary	ironstone (s)	banded iron formation
sedimentary	ironstone (s)	carbonate iron formation
sedimentary	ironstone (s)	carbonate ironstone
sedimentary	ironstone (s)	iron formation
sedimentary	ironstone (s)	ironstone
sedimentary	ironstone (s)	oxide iron formation
sedimentary	ironstone (s)	oxide ironstone
sedimentary	ironstone (s)	silicate iron formation
sedimentary	ironstone (s)	silicate ironstone
sedimentary	ironstone (s)	sulphide iron formation
sedimentary	ironstone (s)	sulphide ironstone
sedimentary	limestone (s)	bafflestone
sedimentary	limestone (s)	bindstone
sedimentary	limestone (s)	boundstone
sedimentary	limestone (s)	calcarenite
sedimentary	limestone (s)	calcilutite
sedimentary	limestone (s)	calcisiltite
sedimentary	limestone (s)	coquina
sedimentary	limestone (s)	crystalline limestone
sedimentary	limestone (s)	floatstone
sedimentary	limestone (s)	framestone
sedimentary	limestone (s)	grainstone
sedimentary	limestone (s)	lime mudstone
sedimentary	limestone (s)	limestone

LITHGROUP	LITHTYPE	LITHDETAIL
sedimentary	limestone (s)	limestone breccia
sedimentary	limestone (s)	marlstone
sedimentary	limestone (s)	micrite
sedimentary	limestone (s)	packstone
sedimentary	limestone (s)	rudstone
sedimentary	limestone (s)	stromatolitic limestone
sedimentary	limestone (s)	wackestone
sedimentary	phosphate (s)	phosphorite
sedimentary	sandstone (s)	arkose
sedimentary	sandstone (s)	arkosic arenite
sedimentary	sandstone (s)	chert arenite
sedimentary	sandstone (s)	feldspathic arenite
sedimentary	sandstone (s)	feldspathic wacke
sedimentary	sandstone (s)	lithic arenite
sedimentary	sandstone (s)	lithic arkose
sedimentary	sandstone (s)	lithic wacke
sedimentary	sandstone (s)	orthoquartzite
sedimentary	sandstone (s)	quartz arenite
sedimentary	sandstone (s)	quartz wacke
sedimentary	sandstone (s)	quartzitic wacke
sedimentary	sandstone (s)	subarkose
sedimentary	sandstone (s)	subchert arenite
sedimentary	sandstone (s)	sublitharenite
sedimentary	siliceous chemical (s)	chert
sedimentary	siliceous chemical (s)	flint
sedimentary	siliceous chemical (s)	jasper
tectonite	brittle (t)	breccia
tectonite	brittle (t)	fault breccia
tectonite	brittle (t)	fault gouge
tectonite	brittle (t)	fault rock
tectonite	brittle (t)	tectonic breccia
tectonite	brittle (t)	tectonic melange
tectonite	brittle hydrothermally altered (t)	fault breccia
tectonite	brittle hydrothermally altered (t)	fault rock
tectonite	brittle-ductile (t)	protomylonite
tectonite	brittle-ductile hydrothermally altered (t)	breccia
tectonite	brittle-ductile hydrothermally altered (t)	fault breccia
tectonite	brittle-ductile hydrothermally altered (t)	mylonite
tectonite	brittle-ductile hydrothermally altered (t)	protomylonite
tectonite	brittle-ductile hydrothermally altered (t)	tectonic breccia
tectonite	ductile (t)	blastomylonite
tectonite	ductile (t)	cataclasite
tectonite	ductile (t)	mylonite
tectonite	ductile (t)	phyllonite
tectonite	ductile (t)	protomylonite
tectonite	ductile (t)	pseudotachylyte
tectonite	ductile (t)	shear zone

LITHGROUP	LITHTYPE	LITHDETAIL
teconite	ductile (t)	ultramylonite
teconite	ductile hydrothermally altered (t)	mylonite
volcanic	felsic (v)	alkali-feld quartz trachyte
volcanic	felsic (v)	alkali-feldspar rhyolite
volcanic	felsic (v)	alkali-feldspar trachyte
volcanic	felsic (v)	comendite
volcanic	felsic (v)	dacite
volcanic	felsic (v)	felsic volcanic rock
volcanic	felsic (v)	felsite
volcanic	felsic (v)	hydrothermally altered
volcanic	felsic (v)	pantellerite
volcanic	felsic (v)	pumice
volcanic	felsic (v)	quartz latite
volcanic	felsic (v)	quartz trachyte
volcanic	felsic (v)	rhyodacite
volcanic	felsic (v)	rhyolite
volcanic	felsic (v)	trachyte
volcanic	felsic (v)	unknown
volcanic	felsic hydrothermally altered (v)	felsic volcanic rock
volcanic	felsic hydrothermally altered (v)	felsite
volcanic	felsic hydrothermally altered (v)	hydrothermally altered
volcanic	felsic hydrothermally altered (v)	rhyolite
volcanic	felsic hydrothermally altered (v)	unknown
volcanic	intermdediate hydrothermally altered (v)	andesite
volcanic	intermdediate hydrothermally altered (v)	intermediate volcanic rock
volcanic	intermdediate hydrothermally altered (v)	unknown
volcanic	intermediate (v)	andesite
volcanic	intermediate (v)	basaltic andesite
volcanic	intermediate (v)	boninite
volcanic	intermediate (v)	diabase
volcanic	intermediate (v)	intermediate volcanic rock
volcanic	intermediate (v)	latite
volcanic	intermediate (v)	quartz andesite
volcanic	intermediate (v)	trachyandesite
volcanic	intermediate (v)	unknown
volcanic	mafic (v)	basalt
volcanic	mafic (v)	komatiitic basalt
volcanic	mafic (v)	mafic volcanic rock
volcanic	mafic (v)	obsidian
volcanic	mafic (v)	trachybasalt
volcanic	mafic (v)	unknown
volcanic	mafic hydrothermally altered (v)	mafic volcanic rock
volcanic	mafic hydrothermally altered (v)	unknown
volcanic	porphyry (v)	feldspar porphyry
volcanic	porphyry (v)	feldspar-quartz porphyry
volcanic	porphyry (v)	mafic phenocrysts
volcanic	porphyry (v)	porphyry, feldspar

LITHGROUP	LITHTYPE	LITHDETAIL
volcanic	porphyry (v)	porphyry, quartz-feldspar
volcanic	porphyry (v)	quartz porphyry
volcanic	porphyry (v)	quartz-feldspar porphyry
volcanic	porphyry (v)	unknown
volcanic	porphyry hydrothermally altered (v)	feldspar porphyry
volcanic	porphyry hydrothermally altered (v)	feldspar-quartz porphyry
volcanic	porphyry hydrothermally altered (v)	porphyry, feldspar
volcanic	porphyry hydrothermally altered (v)	quartz porphyry
volcanic	porphyry hydrothermally altered (v)	quartz-feldspar porphyry
volcanic	porphyry hydrothermally altered (v)	unknown
volcanic	silica undersaturated (v)	basanite
volcanic	silica undersaturated (v)	foidite
volcanic	silica undersaturated (v)	nephelinite
volcanic	silica undersaturated (v)	phonolite
volcanic	silica undersaturated (v)	tephrite
volcanic	ultramafic (v)	komatiite
volcanic	ultramafic (v)	picrite
volcanic	ultramafic (v)	ultramafic lamprophyre
volcanic	ultramafic (v)	ultramafic volcanic rock
volcaniclastic	ash (vc)	ash flow
volcaniclastic	ash (vc)	bentonite
volcaniclastic	ash (vc)	felsic ash tuff
volcaniclastic	ash (vc)	felsic tuff
volcaniclastic	ash (vc)	foid ash tuff
volcaniclastic	ash (vc)	foid tuff
volcaniclastic	ash (vc)	intermediate ash tuff
volcaniclastic	ash (vc)	intermediate tuff
volcaniclastic	ash (vc)	mafic ash tuff
volcaniclastic	ash (vc)	mafic tuff
volcaniclastic	ash (vc)	pumice
volcaniclastic	ash (vc)	ultramafic ash tuff
volcaniclastic	ash (vc)	ultramafic tuff
volcaniclastic	ash hydrothermally altered (vc)	ash flow
volcaniclastic	ash hydrothermally altered (vc)	felsic tuff
volcaniclastic	ash hydrothermally altered (vc)	intermediate tuff
volcaniclastic	ash hydrothermally altered (vc)	mafic tuff
volcaniclastic	bombs (vc)	felsic agglomerate
volcaniclastic	bombs (vc)	foid agglomerate
volcaniclastic	bombs (vc)	intermediate agglomerate
volcaniclastic	bombs (vc)	mafic agglomerate
volcaniclastic	bombs (vc)	scoria
volcaniclastic	bombs (vc)	ultramafic agglomerate
volcaniclastic	bombs hydrothermally altered (vc)	hydrothermally altered
volcaniclastic	bombs hydrothermally altered (vc)	polymict breccia
volcaniclastic	bombs hydrothermally altered (vc)	scoria
volcaniclastic	bombs hydrothermally altered (vc)	volcanic breccia
volcaniclastic	breccia (vc)	felsic pyroclastic breccia

LITHGROUP	LITHTYPE	LITHDETAIL
volcaniclastic	breccia (vc)	felsic tuff breccia
volcaniclastic	breccia (vc)	felsic volcanic breccia
volcaniclastic	breccia (vc)	foiid pyroclastic breccia
volcaniclastic	breccia (vc)	foiid tuff breccia
volcaniclastic	breccia (vc)	foiid volcanic breccia
volcaniclastic	breccia (vc)	intermed pyroclastic breccia
volcaniclastic	breccia (vc)	intermediate tuff breccia
volcaniclastic	breccia (vc)	intermediate volcanic breccia
volcaniclastic	breccia (vc)	mafic pyroclastic breccia
volcaniclastic	breccia (vc)	mafic tuff breccia
volcaniclastic	breccia (vc)	mafic volcanic breccia
volcaniclastic	breccia (vc)	ultramaf pyroclastic breccia
volcaniclastic	breccia (vc)	ultramafic tuff breccia
volcaniclastic	breccia (vc)	ultramafic volcanic breccia
volcaniclastic	breccia (vc)	volcanic breccia
volcaniclastic	lapilli (vc)	felsic lapilli stone
volcaniclastic	lapilli (vc)	felsic lapilli tuff
volcaniclastic	lapilli (vc)	foiid lapilli stone
volcaniclastic	lapilli (vc)	foiid lapilli tuff
volcaniclastic	lapilli (vc)	intermediate lapilli stone
volcaniclastic	lapilli (vc)	intermediate lapilli tuff
volcaniclastic	lapilli (vc)	mafic lapilli stone
volcaniclastic	lapilli (vc)	mafic lapilli tuff
volcaniclastic	lapilli (vc)	ultramafic lapilli stone
volcaniclastic	lapilli (vc)	ultramafic lapilli tuff
volcaniclastic	lapilli (vc)	unknown
volcaniclastic	lapilli hydrothermally altered (vc)	felsic lapilli stone
volcaniclastic	lapilli hydrothermally altered (vc)	felsic lapilli tuff
volcaniclastic	lapilli hydrothermally altered (vc)	hydrothermally altered
volcaniclastic	lapilli hydrothermally altered (vc)	intermediate lapilli tuff
volcaniclastic	volcanic sedimentary (vc)	volcanic conglomerate
volcaniclastic	volcanic sedimentary (vc)	volcanic mudstone
volcaniclastic	volcanic sedimentary (vc)	volcanic sandstone
volcaniclastic	volcanic sedimentary (vc)	volcanic siltstone
volcaniclastic	volcanic sedimentary (vc)	volcaniclastic rock
volcaniclastic	volcanic sedimentary hydrothermally altered (vc)	volcaniclastic rock

Table 2: Mira Geoscience lithological classification scheme (after Parsons et al., 2009)

<b>Master Litho 1</b>	<b>Master Litho 2</b>	<b>Master Litho 3</b>
Igneous	Dyke/Sill	Felsic Dyke/Sill
Igneous	Dyke/Sill	Intermediate Dyke/Sill
Igneous	Dyke/Sill	Mafic Dyke/Sill
Igneous	Dyke/Sill	Ultramafic Dyke/Sill
Igneous	Dyke/Sill	Unspecified Dyke/Sill
Igneous	Hypabyssal	Aplite
Igneous	Hypabyssal	Diabase
Igneous	Hypabyssal	Granophyre
Igneous	Hypabyssal	Kimberlite
Igneous	Hypabyssal	Lamprophyre
Igneous	Hypabyssal	Pegmatite
Igneous	Hypabyssal	Porphyry
Igneous	Hypabyssal	Unspecified Hypabyssal
Igneous	Plutonic	Anorthosite
Igneous	Plutonic	Carbonatite
Igneous	Plutonic	Diorite
Igneous	Plutonic	Gabbro
Igneous	Plutonic	Granite
Igneous	Plutonic	Peridotite
Igneous	Plutonic	Pyroxenite/Hornblendite
Igneous	Plutonic	Syenite
Igneous	Plutonic	Unspecified Plutonic
Igneous	Unspecified Igneous	Unspecified Igneous
Igneous	Volcanic	Andesite
Igneous	Volcanic	Basalt
Igneous	Volcanic	Dacite
Igneous	Volcanic	Komatiite
Igneous	Volcanic	Rhyolite
Igneous	Volcanic	Trachyte
Igneous	Volcanic	Unspecified Volcanic
Igneous	Volcanic Pyroclastic	Obsidian
Igneous	Volcanic Pyroclastic	Pumice
Igneous	Volcanic Pyroclastic	Scoria
Igneous	Volcanic Pyroclastic	Tephra
Igneous	Volcanic Pyroclastic	Tuff/Lapillistone
Igneous	Volcanic Pyroclastic	Unspecified Pyroclastic
Metamorphic	Igneous Protolith	Amphibolite
Metamorphic	Igneous Protolith	Meta-Felsic
Metamorphic	Igneous Protolith	Meta-Intermediate
Metamorphic	Igneous Protolith	Meta-Mafic
Metamorphic	Igneous Protolith	Meta-Ultramafic
Metamorphic	Igneous Protolith	Meta-Volcanic
Metamorphic	Igneous Protolith	Orthogneiss
Metamorphic	Igneous Protolith	Orthoschist
Metamorphic	Igneous Protolith	Serpentinite
Metamorphic	Igneous Protolith	Soapstone
Metamorphic	Metasomatic & Contact	Hornfels
Metamorphic	Metasomatic & Contact	Rodingite
Metamorphic	Metasomatic & Contact	Skarn
Metamorphic	Sedimentary Protolith	Argillite
Metamorphic	Sedimentary Protolith	Marble
Metamorphic	Sedimentary Protolith	Meta-Carbonate
Metamorphic	Sedimentary Protolith	Meta-Conglomerate
Metamorphic	Sedimentary Protolith	Meta-Sediment
Metamorphic	Sedimentary Protolith	Paragneiss
Metamorphic	Sedimentary Protolith	Paraschist
Metamorphic	Sedimentary Protolith	Phyllite
Metamorphic	Sedimentary Protolith	Psammitite



**Enkin et al.: Physical Property Measurements at the GSC - Table 2**

<b>Master Litho 1</b>	<b>Master Litho 2</b>	<b>Master Litho 3</b>
Metamorphic	Sedimentary Protolith	Quartzite
Metamorphic	Sedimentary Protolith	Slate
Metamorphic	Unknown Protolith	Eclogite
Metamorphic	Unknown Protolith	Gneiss
Metamorphic	Unknown Protolith	Granulite
Metamorphic	Unknown Protolith	Greenstone
Metamorphic	Unknown Protolith	Migmatite
Metamorphic	Unknown Protolith	Mylonite
Metamorphic	Unknown Protolith	Schist
Metamorphic	Unspecified Metamorphic	Unspecified Metamorphic
Other	Mineralized/Alteration	Alteration Zone
Other	Mineralized/Alteration	Graphite
Other	Mineralized/Alteration	Mineralized Zone
Other	Ore/Metals	Metals
Other	Ore/Metals	Ore
Other	Structure	Breccia(ed)
Other	Structure	Fault(ed)
Other	Structure	Fracture(d)
Other	Structure	Shear(ed)
Other	Structure	Vein(ed)
Other	Sulphide/Oxide	Disseminated Sulphide
Other	Sulphide/Oxide	Massive Sulphide
Other	Sulphide/Oxide	Oxide
Other	Sulphide/Oxide	Sulphide
Other	Tectonic	Cataclasite
Sedimentary	Carbonate	Dolostone
Sedimentary	Carbonate	Limestone
Sedimentary	Carbonate	Unspecified Carbonate
Sedimentary	Chemical Silicate	Chert
Sedimentary	Chemical Silicate	Diatomite
Sedimentary	Chemical Silicate	Porcellanite
Sedimentary	Chemical Silicate	Unspecified Chemical Silicate
Sedimentary	Evaporite	Anhydrite
Sedimentary	Evaporite	Gypsum
Sedimentary	Evaporite	Potash
Sedimentary	Evaporite	Rock Salt
Sedimentary	Evaporite	Trona
Sedimentary	Evaporite	Unspecified Evaporite
Sedimentary	Iron-Rich	Iron Formation
Sedimentary	Iron-Rich	Ironstone
Sedimentary	Iron-Rich	Unspecified Iron-Rich
Sedimentary	Organic	Coal
Sedimentary	Organic	Oil Sand
Sedimentary	Organic	Oil Shale
Sedimentary	Organic	Peat
Sedimentary	Organic	Petroliferous Sandstone
Sedimentary	Organic	Unspecified Organic
Sedimentary	Siliciclastic	Arenite
Sedimentary	Siliciclastic	Arkose
Sedimentary	Siliciclastic	Claystone
Sedimentary	Siliciclastic	Conglomerate
Sedimentary	Siliciclastic	Pelite
Sedimentary	Siliciclastic	Sandstone
Sedimentary	Siliciclastic	Shale
Sedimentary	Siliciclastic	Siltstone
Sedimentary	Siliciclastic	Unspecified Siliciclastic
Sedimentary	Siliciclastic	Wacke
Sedimentary	Unconsolidated	Clay
Sedimentary	Unconsolidated	Gravel
Sedimentary	Unconsolidated	Mud

<b>Master Litho 1</b>	<b>Master Litho 2</b>	<b>Master Litho 3</b>
Sedimentary	Unconsolidated	Overburden
Sedimentary	Unconsolidated	Sand
Sedimentary	Unconsolidated	Silt
Sedimentary	Unconsolidated	Tailings
Sedimentary	Unconsolidated	Till
Sedimentary	Unconsolidated	Unspecified Sediment
Sedimentary	Unspecified Sedimentary	Unspecified Sedimentary
Unknown	Unknown	Unknown